Geophysical Journal International

Geophys. J. Int. (2023) **232,** 884–901
Advance Access publication 2022 September 17
GJI Gravity, Geodesy and Tides

https://doi.org/10.1093/gji/ggac365

Can GPS and GRACE data be used to separate past and present-day surface loading in a data-driven approach?

Yann Ziegler,[1] Bramha Dutt Vishwakarma,[1,2] Aoibheann Brady,[1,3] Stephen Chuter,[1] Sam Royston,[1] Richard M. Westaway[1] and Jonathan L. Bamber[1,4]

[1]*Bristol Glaciology Centre, School of Geographical Sciences, University of Bristol, University Road, BS*81*SS Bristol, United Kingdom.*
E-mail: y.ziegler@bristol.ac.uk
[2]*Interdisciplinary Centre for Water Research, Indian Institute of Science, Bengaluru, Karnataka* 560012*, India*
[3]*Centre for Earth Sciences, Indian Institute of Science, Bengaluru, Karnataka* 560012*, India*
[4]*Department of Aerospace and Geodesy, Data Science in Earth Observation, Technical University of Munich,* 80333 *München, Germany*

Accepted 2022 September 15. Received 2022 September 6; in original form 2021 September 23

SUMMARY

Glacial isostatic adjustment (GIA) and the hydrological cycle are both associated with mass changes and vertical land motion (VLM), which are observed by GRACE and GPS, respectively. Hydrology-related VLM results from the instantaneous response of the elastic solid Earth to surface loading by freshwater, whereas GIA-related VLM reveals the long-term response of the viscoelastic Earth mantle to past ice loading history. Thus, observations of mass changes and VLM are interrelated, making GIA and hydrology difficult to quantify and study independently. In this work, we investigate the feasibility of separating these processes based on GRACE and GPS observations, in a fully data-driven and physically consistent approach. We take advantage of the differences in the spatio-temporal characteristics of the GIA and hydrology fields to estimate the respective contributions of each component using a Bayesian hierarchical modelling framework. A closed-loop synthetic test confirms that our method successfully solves this source separation problem. However, there are significant challenges when applying the same approach with actual observations and the answer to the main question of this study is more nuanced. In particular, in regions where GPS station coverage is sparse, the lack of informative data becomes a limiting factor.

Key words: Loading of the Earth; Time variable gravity; Satellite geodesy; Hydrology; Joint inversion; Statistical methods.

1 INTRODUCTION

1.1 Past and present-day surface loading

The Earth responds to large mass changes occurring at its surface by changing its shape, gravity field and rotation. This response depends on the nature and spatio-temporal characteristics of the surface processes, as well as on the Earth structure and properties.

The loading and unloading of the Earth surface at subdecadal periods (or present-day surface mass load, PDSML) induces instantaneous, elastic deformations of the Earth surface and changes in the geopotential. In particular, vertical land motions (VLM) due to such an elastic deformation have been routinely observed in relation with current mass change at the surface (van Dam *et al.* 2001; Tregoning *et al.* 2009; Nordman *et al.* 2009; Fritsche *et al.* 2012; Adusumilli *et al.* 2019). The relation between hydrological mass change and the induced elastic VLM field is non-local in the sense that it involves a spatial convolution between surface mass change and the Earth Green's function for the vertical displacement in response to a point surface load (Farrell 1972). Assuming a purely elastic deformation, the Green's function essentially depends on the elastic load Love numbers (LLN) h'_ℓ, where ℓ is the harmonic degree in the spherical harmonic decomposition of the displacement field, and the LLN are completely defined by the Earth properties.

At short timescales, the contribution of the viscous deformation of the Earth mantle to the total displacement in response to a load remains small (Peltier 1974), which justifies the elastic response assumption [except in areas of very low mantle viscosity such as West Antarctica (van der Wal *et al.* 2015) and Southeast Alaska (Hu & Freymueller 2019)]. At much longer timescales, however, it becomes essential to consider the contribution of the viscous response of the mantle. Past surface loading differs from present-day loading because the associated mass changes which can be directly observed today are from fundamentally different origins. With present-day loading, observed mass change is due to the load itself, whereas current mass change observed after past loading is

due to the motion of viscous and dense mantle materials occurring at depth. Although well-known in theory, this fact is still a challenge in practice because it makes the separation of past and present-day surface loading a difficult problem.

1.2 GIA and hydrology observed by space geodetic techniques

Geodetic sensors such as satellite gravimetry, global navigation satellite system (GNSS) and satellite laser ranging have been instrumental in mapping the mass redistribution near the surface of the Earth. The total signal observed by these geodetic sensors has been approximately attributed to known processes with the help of geophysical models. Separating these underlying processes in a data-driven framework is still a challenge, however.

In this work, we focus on separating the signals from two major processes: the glacial isostatic adjustment (GIA), which is the response of the Earth to past ice loading history, and present-day land hydrology and ice mass balance, which governs surface loading changes due to freshwater. We include in this study both liquid water stored in aquifers, lakes, rivers, etc., and frozen water such as snow cover and glaciers. We ignore long-term trends in hydrology (centennial scales and above), which may also trigger a viscous response. Both major processes induce VLM and changes in the Earth geopotential, which can be, respectively, observed by GNSS techniques, such as GPS, and gravity field measurement missions, such as GRACE (e.g. van Dam *et al.* 2001; Fritsche *et al.* 2012; Husson *et al.* 2018).

Hydrology-related loading occurs during the seasonal or secular accumulation of freshwater (including groundwater) in basins, whereas unloading occurs when freshwater leaves the basins through natural outflows, evapotranspiration and snow and ice melting. Other phenomena may induce the redistribution of freshwater in a catchment or at larger scale without an immediate change in local surface load (anthropogenic groundwater pumping or river water abstraction for irrigation, for example), or may induce VLM without changing the volume of water stored in a basin (poroelasticity, for example). When they are non-negligible, these should be dealt with separately as they are different from viscoelastic surface loading.

Locally, when GRACE observes an increase in terrestrial water storage (TWS), GNSS techniques observe a downward land motion, or negative VLM. Conversely, drought periods correspond to a decrease in TWS as observed by GRACE and to a positive VLM as seen by GNSS. This inverse relationship between GRACE and GNSS observations is the signature of an elastic deformation due to PDSML.

By contrast, glacial and interglacial periods are long-term events during which the mantle can accumulate and return large viscous deformations following loading and unloading by ice sheets. That being said, GIA is more than the viscous counterpart of the purely elastic deformation due to PDSML; as stated earlier, there is a more fundamental distinction between both processes. Whereas there is a causal relation between surface loading by freshwater during hydrology cycles and the resulting VLM, such a view does not identically apply to present-day GIA-related mass change. The upward viscous motion of deeper and denser materials, and the simultaneous land motion, which is observed at the Earth surface, should be seen as two components of the same process, namely the delayed, dynamical adjustment of the solid Earth to a new loading state. Contrary to PDSML, GIA is a delayed response of surface mass changes which happened decades to thousands of years ago and which are not directly available to us from contemporary observations. Detailed palaeogeographic reconstructions of ancient ice sheets are still possible (Clayton & Moran 1982; Dyke 2004; Margold *et al.* 2018) but those are models inferred from field observations. The causal Green's function approach may be used to relate contemporary mass changes to VLM (similarly to what is done when relating PDSML to elastic VLM) but, for GIA, it requires assumptions and approximations on ice loading history. This is what is done in GIA forward models such as Peltier *et al.* (2015). Thus, any fully data-driven estimation of GIA-related VLM from observed contemporary mass change remains a challenge.

This fundamental difference between PDSML and GIA has both theoretical and practical implications (Chao 2016), for example when interpreting geodetic observations. With GIA, when GRACE observes an increase in mass locally, GNSS techniques observe an upward land motion, or positive VLM, at the same location. Conversely, in the peripheral region of the main GIA bulges, where VLM is negative, GRACE observes a negative mass change. Such a direct relationship between GRACE and GNSS observations is the signature of a viscous deformation due to GIA (or to another delayed process). Furthermore, GRACE measured mass changes are usually expressed either as a geopotential anomaly or in units of millimetres water-height equivalent, while VLM is in units of distance. Ideally, to solve for the two underlying processes (GIA and hydrology) from the two data sets in spatial domain, the observations should be given in the same physical quantity, such as millimetres of VLM. To achieve this, GRACE measurements should be transformed into VLM. Such transformation is unfortunately not a simple conversion or pointwise mapping but a convolution in the spatial domain, for which the fraction of the total mass change from GIA (viscous process) or from hydrology (elastic process) must be known, which actually is the problem to be solved.

1.3 Statistical challenges in separating the past and present-day surface loading

If it were possible to make precise measurements of mass and elevation at a specific location on the Earth's surface, annually over several decades, we would likely see a smooth dominantly linear trend with subdecadal excursions in each time-series. The trend represents GIA and secular changes in hydrology, while the excursions are mainly intra/interannual hydrological processes. Separating out GIA and hydrology is crucial for understanding the physics of the Earth's mantle, for paleoclimate reconstruction, and for projecting the effects of climate change on hydrology (Tapley *et al.* 2019).

Unfortunately, we do not have these measurements at a satisfactory spatio-temporal resolution. Instead, we have GRACE measurements of monthly mass change at a coarse spatial resolution (approximately 65 000 km^2; Vishwakarma *et al.* 2018), and GPS measurements of elevation at specific locations, which are irregularly distributed in space, and can change through the time period. The GPS measurements are high-resolution in time, but can be transformed into changes in monthly averages, to give annual VLM to match the time intervals of the GRACE measurements.

As it stands, this sounds like a challenging but recognisable statistical problem. There are two latent spatio-temporal processes: first, changes due to GIA, which we can treat as effectively time-invariant on a timescale of a few decades; secondly, changes due to hydrology, which varies in space and time. We expect that both of these processes would be fairly smooth, and that the spatial

correlation length of GIA (crudely, the spatial stiffness of the latent process) would be longer than that of hydrology. Then we have two sets of measurements which are known functions of the two latent processes: GRACE annual mass change, and GPS annual VLM.

This is a standard statistical model, in which the modelling runs 'forward' from the latent processes to the measurements; usually termed a 'state space model'. Bayesian updating handles the inverse problem, of passing information 'backwards' from the measurements to the latent processes. This also requires a prior distribution on the latent processes, which is where we can constrain the spatial correlation lengths. Often this prior distribution is specified conditionally on some hyperparameters, where uncertainty in these hyperparameters allows for considerable vagueness in the prior distribution, but requires a more sophisticated statistical treatment.

At first glance, this statistical approach ought to perform well, in separating the GIA and hydrology processes. As explained in Section 1.2, these two processes are expected to have different signatures in the observations. Furthermore, they have different spatial correlation lengths, and GIA is effectively time-invariant. The main challenge, from a statistical point of view, is shortness in the measurement period. If we only have a decade of measurements, then the hydrology at some locations will appear linear, and could be confused with the GIA signal. The main strategy to defeat this is to take into account the difference in spatial correlation lengths between GIA and hydrology, but this is a soft constraint and may not be enough to overcome measurement error and sparsity in GPS measurements.

1.4 Past attempts

As stated in Section 1.2, the relationships between GRACE and GNSS observations, in the contrasting cases of an elastic or viscous response, are only valid locally. In addition, they only hold when a single process is involved. At larger spatial scales, and/or when GIA and hydrological signals are colocated, the separation of past and present-day surface loading can be challenging or even impossible if the differences in the spatio-temporal characteristics of the processes are similar and not specifically handled.

The work of Sella *et al.* (2007) is such an example of a GIA estimate where PDSML is implicitly assumed to be negligible over the region of interest. In their study on GRACE data, van der Wal *et al.* (2008) highlight the importance of the uncertainties in hydrology models when estimating GIA in North America and mention the fact that 'for the purpose of studying GIA, the use of numerical hydrology models is inevitable' due to the lack of global observations of soil moisture. The main problem here is that both GIA and changes in TWS can exhibit linear trends over the period of observation. Of course, PDSML is not the only source of errors in GIA estimates. For example, the impact of 3-D structures in the Earth mantle on GIA is an active field of research (Geruo *et al.* 2012; Li *et al.* 2020; Marsman *et al.* 2021).

Conversely, Booker *et al.* (2014) provide a global estimate of secular surface mass loading where GIA is assumed to be known, although the limitations in the accuracy of the selected GIA models is clearly recognised. Indeed, choosing a GIA model and subtracting it from GRACE or GNSS observations is not necessarily a problem when focusing on subannual seasonal changes in PDSML, but there is a risk of biasing the results when estimating decadal or secular components.

In response to these challenges, new studies have been dedicated to the separation and simultaneous estimation of land motion, mass change or sea level and their different components observed by various geodetic techniques. Several data-driven inversions have solved for the Stokes coefficients in the spherical harmonic domain (Wu *et al.* 2010; Rietbroek *et al.* 2016) whilst others have made local approximations on the ratio of densities of the solid rock to ice to circumvent the challenge of source separation between past and present-day surface loading (Riva *et al.* 2009; Gunter *et al.* 2014; Martín-Español *et al.* 2016). The work of Vishwakarma *et al.* (2022) is one of the most recent step in that direction, providing a global solution for both GIA and PDSML; we shall refer frequently to this study as we share the same strategy (see Section 2).

1.5 Overview of this work

This work is part of a larger project, GlobalMass, which aims at attributing sea level rise to its component parts. In this context, having a proper and consistent global estimate of VLM due to GIA and hydrology is of particular importance. The present study is another iteration in that direction. In particular, it follows the work of Sha *et al.* (2018) and Schumacher *et al.* (2018) on global GIA fields.

The goal of this work is twofold. First, we develop a new, generic method to separate VLM fields due to past and present-day surface loading in a data-driven approach. Here, we implicitly consider that being 'data-driven' means, loosely speaking, that the main driving factor of our results should be the input data and not some fixed (hyper)parameters in our inversion framework or a chosen set of assumptions and geophysical models. Our method is fully described in Section 2. Its main components are provided in Section 2.1, along with a summary of a related approach where the data-driven constraint is relaxed, for illustrative purposes. We detail the key idea of the method, which is a specific transformation of GRACE observations, in Section 2.2, before providing a complete mathematical description of the method in Section 2.3.

Our secondary goal is to apply this method using GRACE and GPS observations to provide a new, data-driven estimate of the VLM fields due to GIA and PDSML (mostly due to hydrology), with a focus on North America for the decade 2005–2015, which is fully covered by GRACE data. As expected, one of the biggest challenges is the source separation problem described in previous sections, particularly since on a time period of a decade, some long-term hydrological processes may exhibit a linear behaviour similar to the GIA-induced displacements. The actual implementation of our framework is described in Section 3.1. To validate our method and code, we run a synthetic test in Section 3.2 and provide the results in Section 3.3. Then, we apply the method to actual GRACE and GPS observations in Section 3.4 and provide the results in Section 3.5.

We discuss the results in Section 4. The overall validity of our approach is assessed in Section 4.1 thanks to the synthetic test results and we discuss the results and potential improvements when using real-world observations in Section 4.2. The main caveats of the method are considered in Section 4.3 before concluding in Section 5.

2 METHOD

2.1 Overview

The simultaneous estimation of GIA and PDSML-related VLM fields requires a geophysically consistent framework where the observations are properly related to each process, taking into account their different physical nature (Section 1.2). Our goal is precisely to separate these processes and provide a reliable estimate of the time-invariant GIA (constant linear trend) and time-evolving hydrology fields.

There are two main challenges here. At the observational level, there is a modelling challenge because we need to combine different physical quantities: displacements observed by GNSS techniques and mass changes observed by GRACE. As stated in Section 1.2, the transformation from one quantity to another is a non-trivial problem. It depends on the Earth physical characteristics and, even more importantly, it requires, in theory, the separation of hydrology from GIA, which is the problem we are trying to solve. The second challenge is the source separation itself. Both GIA and hydrology processes contain large scale, long-term signals and exhibit linear trends, which make them,in principle, impossible to separate unless extra geophysical information is provided. Thus, since both challenges are tightly intertwined, we need a method which addresses them simultaneously.

The usual approach relies on the dubious assumption that only one process is observed at a time and that all other processes have been removed using appropriate corrections, or that each process has its own, non-overlapping temporal characteristics. If we want to go beyond these assumptions, we can take advantage of the differences between what GRACE and GNSS techniques observe. At a very high level, the approach could be as follows. If we suppose that the GIA model is perfect, after removing it from both observed mass change (from GRACE) and VLM (from GNSS), the remaining signals in each data set would have opposite signs and amplitudes consistent with hydrology-related elastic loading. Such consistency would reveal that the GIA correction is zero and that the observed signal is from hydrology; then the latter can easily be extracted from either data set. If the GIA model is not perfect, however, there will be inconsistencies between GRACE and GNSS observations when interpreted in terms of hydrological signal. For example, an underestimated GIA amplitude in the model could result in a positive VLM (due to uncorrected GIA uplift) associated with positive mass change, which cannot be the result of hydrological loading. From such inconsistencies, we should be able to estimate a GIA correction to improve the original model and, by implication, also an hydrology field consistent with the GIA signal. Obviously, the real challenge is to put this general idea in practice.

To do so, we have at least two different kinds of strategies. One of them is data-driven only in a wider sense because it embeds more physics than what we would aim at in a fully data-driven approach, making for a slightly more 'knowledge-driven', or physics-based approach. It uses the least squares method and has been recently followed by (Vishwakarma *et al.* 2022). The cornerstone of this method is to compute the difference between GNSS-observed VLM and GRACE-derived VLM, using physical models for the transformation from mass change to VLM for GRACE and assuming that GRACE observes either *only* an elastic deformation or *only* a viscous deformation of the Earth surface (both of them having different physical signatures as explained in Section 1.2). In both cases, such an assumption is wrong for one of the GRACE component/process and a correcting term is added in the model equation to counterbalance that erroneous term. The result of this computation is either the GIA or hydrology field, depending on the chosen GRACE data transformation and its corresponding counter-correction. This method is effective but directly relies on physical laws which require the computation of convolutions in the spatial domain as there is no accurate local equation which relates mass change to VLM (Section 1.1). That is why Vishwakarma *et al.* (2022) work in spatial frequency domain, with spherical harmonics coefficients, where the inversion is reduced to a linear algebra problem (but still requires geophysical laws to relate the observed quantities to the unknowns).

The other approach, summarized on Fig. 1, is the one we use in this work. It takes advantage of the generic Bayesian hierarchical modelling (BHM) approach described in Section 3.1. It is data-driven in the sense that we do not rely on any specific physical law at the BHM level, apart from the very simple relation:

$$\text{total VLM} = \text{time-evolving VLM} + \text{time-invariant VLM}, \qquad (1)$$

which is nothing but the superposition principle applied to VLM due to hydrology and GIA. The first challenge, regarding the transformation from mass change to VLM, is split in two here. First, we approximate the solution of the source separation problem with a GIA forward model which we remove from GRACE observations before applying the transformation, assuming a viscous response of the solid Earth. This step is similar to the first step of the aforementioned approach of Vishwakarma *et al.* (2022) and results in what we call the *pseudo-GRACE product*. The motivations and equations behind the pseudo-GRACE product are detailed in Section 2.2. At this point, all the input data (pseudo-GRACE product and GPS) are given in terms of VLM and can be used by the BHM after a few additional pre-processing steps. Then, we need to handle the discrepancy between the actual GIA field and the GIA prior (used in the pseudo-GRACE product computation and as an implicit prior in the BHM) with great care, both at the BHM level and in an additional post-BHM processing step, because this discrepancy will be different in the pseudo-GRACE product from the one in the GPS data. Indeed, the pseudo-GRACE product computation erroneously (but purposely) transforms the deviation from the GIA prior into an elastic deformation, which is of course different from what GNSS techniques observe. The aforementioned post-BHM processing step is simply the inverse of the transformation we applied to compute the pseudo-GRACE product, followed by the computation of VLM from mass change. This step is depicted by the last box of Fig. 1. Once again, the cornerstone of the method is to take that difference between GRACE and GNSS observations into account in the design of the framework instead of trying to remove it by making unsatisfactory assumptions.

Thus, in the approach we use in this work, we actually estimate two time-invariant GIA-induced VLM fields (one from GRACE observations, one from GPS) and one time-evolving hydrology-induced VLM field, which is common to both observing techniques. The time-invariant VLM field estimated from pseudo-GRACE data is actually a pseudo-GIA field in the sense that it is a proxy which describes the GIA signal but does not directly represent the GIA-induced VLM field. It must be transformed before being compared or combined with the GIA VLM field estimated from GPS observations [see output post-processing for option (a) on Fig. 1]. The next sections will make all these steps more explicit and provide further explanations.

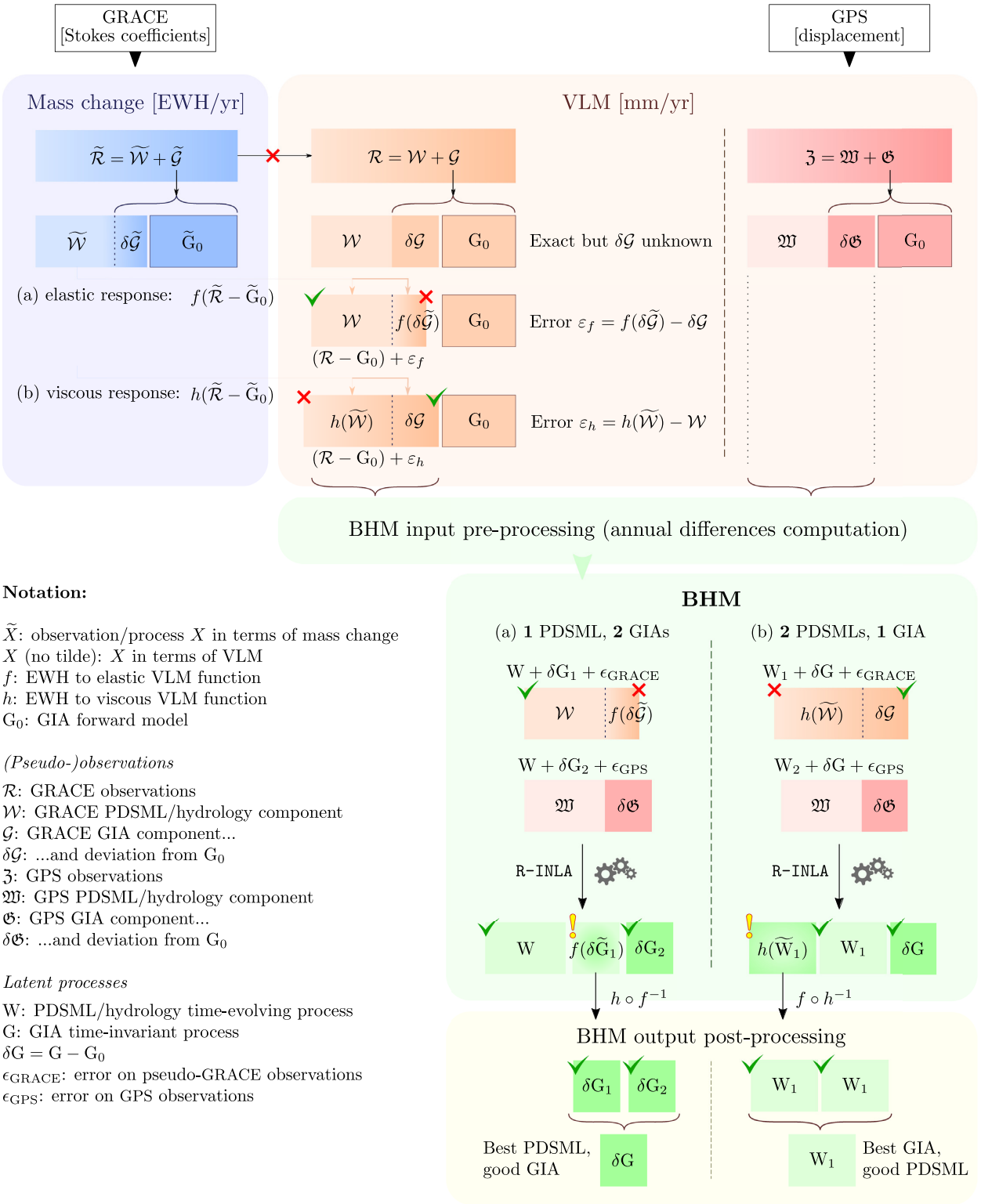

Figure 1. From observations to final PDSML and GIA related VLM estimates. This figure might also be useful to find the meaning of a symbol used in the main text and to visually understand the physical meaning of the corresponding quantity. Options (a) and (b) are explained in the main text; the numbers in front of 'PDSML' and 'GIA' at the top of the main green box indicate the number of processes used in the BHM for each approach. Red crosses indicate non-physical quantities (for example, elastic VLM computed from GIA-related mass change), contrary to green ticks. Yellow exclamation points also indicate non-physical quantities estimated from GRACE data, but those can be used as a proxy to estimate VLM due to GIA (a) or PDSML (b) in a post-processing step (see Section 2.3). `R-INLA` refers to the `R` package we use to do the Bayesian inference (Rue *et al.* 2009, r-inla.org).

2.2 The pseudo-GRACE product

In order to solve for the two processes, the observations should describe the same physical quantities with the same units, i.e. we need to transform mass change to VLM (or the other way around, VLM to mass change, which would introduce the same challenges). Only then can we combine GRACE and GPS data in the BHM. Note that we compute year-to-year rate of change for each quantity and exclusively work with these derived rates instead of the original mass change and displacement. The motivations underlying this choice are discussed in Section 3.1; for our purpose it is essentially a way to remove the trends from time-series.

We assume the surface of the Earth to be the sphere $\mathbb{S}^2$ and work in the domain $\mathcal{D} \subset \mathbb{S}^2$. As usual, $\mathbb{R}$ is the set of real numbers. Following Vishwakarma *et al.* (2022) notations, let $\Delta\dot{u}$ be the *VLM function* which gives the VLM at position $s \in \mathcal{D}$ (for example, in mm yr^{-1}):

$$\begin{aligned} \Delta\dot{u} : \mathcal{D} &\to \mathbb{R} \\ s &\mapsto \Delta\dot{u}(s). \end{aligned} \tag{2}$$

Similarly, let $\Delta\dot{m}$ be the *mass change rate function* which gives the mass change rate at position s (for example, in kg m^{-2} yr^{-1} or in equivalent water height EWH, mm WE yr^{-1}):

$$\begin{aligned} \Delta\dot{m} : \mathcal{D} &\to \mathbb{R} \\ s &\mapsto \Delta\dot{m}(s). \end{aligned} \tag{3}$$

GNSS observations provide a sparse spatial sampling of $\Delta\dot{u}(s)$, whereas GRACE provides a continuous spatial sampling of $\Delta\dot{m}(s)$. From a physical point of view, $\Delta\dot{u}$ and $\Delta\dot{m}$ are not independent of each other because they describe different aspects of the same set of geophysical processes (Section 1.2).

It is physically impossible, for a given $s_0 \in \mathcal{D}$, to compute $\Delta\dot{u}(s_0)$ from $\Delta\dot{m}(s_0)$ as there is no local relation between these physical quantities (Section 1.1). In theory, we need to know $\Delta\dot{m}(s)$ for all $s \in \mathbb{S}^2$, or at least for all $s \in \mathcal{D}$, to properly compute $\Delta\dot{u}(s_0)$. Here we implicitly assume that VLM is entirely due to mass changes and that no other processes come into play.

Let f and h be the functionals which map $\Delta\dot{m}$ to $\Delta\dot{u}(s_0)$, assuming an instantaneous elastic or delayed viscoelastic response of the Earth, respectively:

$$f : \Delta\dot{m} \mapsto \Delta\dot{u}(s_0) = \int_{\mathcal{D}} \Delta\dot{m}(s) F(s_0 - s)\, \mathrm{d}s \tag{4}$$

and

$$h : \Delta\dot{m} \mapsto \Delta\dot{u}(s_0) = \int_{\mathcal{D}} \Delta\dot{m}(s) H(s_0 - s)\, \mathrm{d}s, \tag{5}$$

where F is the Green's function relating short-term (elastic) loading and unloading at the Earth surface to VLM and H is the Green's function relating long-term (viscous) mass changes due to GIA to VLM. Let us write GRACE observations as

$$\widetilde{\mathcal{R}} = \widetilde{\mathcal{W}} + \widetilde{\mathcal{G}}, \tag{6}$$

with $\widetilde{\mathcal{W}}$ the mass change, observed by GRACE, due to hydrology and $\widetilde{\mathcal{G}}$ the mass change, observed by GRACE, due to GIA (a tilde means that the quantity describes EWH or mass change). If we already know $\widetilde{\mathcal{W}}$ and $\widetilde{\mathcal{G}}$ accurately, we could apply f and h to each components, respectively, and we would get a physically correct GRACE product in terms of VLM:

$$\begin{aligned} \mathcal{R} &= f\left(\widetilde{\mathcal{W}}\right) + h\left(\widetilde{\mathcal{G}}\right) \\ &= \mathcal{W} + \mathcal{G}, \end{aligned} \tag{7}$$

Table 1. Relation between GRACE observations as mass change and output of the mass change-to-VLM functions, along with actual VLM. For the sake of simplicity, we assume here that only one process is observed at a given location.

	GRACE observations (f or h input)	
	$\widetilde{\mathcal{R}} > 0$ (mass gain)	$\widetilde{\mathcal{R}} < 0$ (mass loss)
Hydrology-induced		
Actual	VLM < 0	VLM > 0
Computed	$f(\widetilde{\mathcal{W}}) < 0$	$f(\widetilde{\mathcal{W}}) > 0$
	$h(\widetilde{\mathcal{W}}) \gtrsim 0$	$h(\widetilde{\mathcal{W}}) \lesssim 0$
GIA-induced		
Actual	VLM > 0	VLM < 0
Computed	$f(\widetilde{\mathcal{G}}) \lesssim 0$	$f(\widetilde{\mathcal{G}}) \gtrsim 0$
	$h(\widetilde{\mathcal{G}}) > 0$	$h(\widetilde{\mathcal{G}}) < 0$

using the definitions

$$\mathcal{W} = f\left(\widetilde{\mathcal{W}}\right) \quad \text{and} \quad \mathcal{G} = h\left(\widetilde{\mathcal{G}}\right). \tag{8}$$

The correspondence between these GRACE-specific notations and the generic notations used in eqs (2)–(5) is: $\widetilde{\mathcal{W}} = \Delta\dot{m}_{\text{hydro}}$ and $\mathcal{W} = \Delta\dot{u}_{\text{elastic}}$ for hydrology, and $\widetilde{\mathcal{G}} = \Delta\dot{m}_{\text{GIA}}$ and $\mathcal{G} = \Delta\dot{u}_{\text{viscous}}$ for GIA.

In practice GRACE observes a total of $\widetilde{\mathcal{W}}$ and $\widetilde{\mathcal{G}}$, therefore, we can only transform the GRACE data to VLM with either f or h and we make an error in one of the components. Table 1 relates the sign of the output of f and h to the sign of their input, depending on the geophysical process involved (locally), and provides a comparison with actual VLM. When correctly using f to compute hydrology-induced VLM or h for GIA-induced VLM, the computed value has the same sign as the actual VLM (blue), although the value may be slightly different due to errors in GRACE observations. On the contrary, when wrongly using f to compute GIA-induced VLM or h for hydrology-induced VLM, the computed value has the opposite sign and an underestimated amplitude compared with the actual VLM (red). This fact alone explains why we cannot use a single constant factor to do the conversion from mass change to VLM, which is in essence not just a conversion but a data transformation through physics-based modelling. It also highlights the importance of the counter-correcting term mentioned in Section 2.1.

Thus, we need to find a way of approximating $\mathcal{R}$ from $\widetilde{\mathcal{R}}$ even though $\mathcal{R}$ is neither equal to $f(\widetilde{\mathcal{R}})$ nor $h(\widetilde{\mathcal{R}})$ in the general case. The starting point of the pseudo-GRACE product computation is the functional f defined in eq. (4), which depends on the chosen earth model and transforms surface water mass change into VLM, assuming an instantaneous elastic response of the Earth. We know that, when applying this function to GRACE observations, we will not properly convert the part of the signal due to GIA because GIA is a viscoelastic process (see Table 1). The key is to handle this inevitable error properly.

The transformations we apply to the original GRACE data are listed hereafter on the left-hand side of what we will call the *pseudo-GRACE product equation*; the result appears on the right-hand side. The first two steps of the computation are:

(i)As f is linear, we can write $f(\widetilde{\mathcal{R}}) = f(\widetilde{\mathcal{W}}) + f(\widetilde{\mathcal{G}})$, using definition (6).
(ii)Then, we know that $\mathcal{W} = f(\widetilde{\mathcal{W}})$, from definition (8), but $\mathcal{G} \neq f(\widetilde{\mathcal{G}})$. So, we can only simplify the previous relation to $f(\widetilde{\mathcal{R}}) = \mathcal{W} + f(\widetilde{\mathcal{G}})$.

The third step would be

(i)$f(\widetilde{\mathcal{R}}) + \mathcal{G} = \mathcal{W} + \mathcal{G} + f(\widetilde{\mathcal{G}})$

to get the $\mathcal{W}+\mathcal{G}=\mathcal{R}$ term we are looking for (a physically correct VLM field from GRACE observations), but it should be clear from the previous sections that we have no practical way to determine $\mathcal{G}$ to add it on the left-hand side of the equation or even to compute $f(\widetilde{\mathcal{G}})$ and remove it from the right-hand side, otherwise our source separation problem would be completely solved already. Instead, we have no other choice here but to use approximations of $\mathcal{G}$ and $\widetilde{\mathcal{G}}$.

Note that these problems are tackled differently in Vishwakarma *et al.* (2022) because, in their study, GPS data are used to directly estimate $\mathcal{W}+\mathcal{G}$ and the spherical harmonic decomposition makes the combination of $\mathcal{G}$ and $f(\widetilde{\mathcal{G}})$ in a single term trivial. As a result, it was possible to solve for $\mathcal{G}$ directly. Such an approach could be adapted to the BHM but for various reasons discussed in Appendix A, it would be suboptimal here.

Let G_0 and $\widetilde{\mathrm{G}}_0$, depending on the physical quantity in use (VLM or mass change), be the prior mean field for GIA, given by a forward model such as ICE-6G (Peltier *et al.* 2015). Then, $\delta\widetilde{\mathcal{G}}$ and $\delta\mathcal{G}$ are the deviations between the GIA component of GRACE data and the chosen GIA model, that is to say:

$$\widetilde{\mathcal{G}} = \widetilde{\mathrm{G}}_0 + \delta\widetilde{\mathcal{G}} \tag{9a}$$

$$\mathcal{G} = \mathrm{G}_0 + \delta\mathcal{G}. \tag{9b}$$

Thus, making the approximation $\mathcal{G} \approx \mathrm{G}_0$, using eq. (9a), and taking advantage of the linearity of f, what we can compute, in practice, is

(iii) $f(\widetilde{\mathcal{R}}) + \mathrm{G}_0 - f(\widetilde{\mathrm{G}}_0) = \mathcal{W} + \mathrm{G}_0 + f(\delta\widetilde{\mathcal{G}})$.
(iv) Finally, we make the GRACE-derived VLM term $\mathcal{W}+\mathcal{G}=\mathcal{R}$ appear by adding and removing $\delta\mathcal{G}$ on the right-hand side:

$$\begin{aligned} f\left(\widetilde{\mathcal{R}}\right) + \mathrm{G}_0 - f\left(\widetilde{\mathrm{G}}_0\right) &= \mathcal{W} + (\mathrm{G}_0 + \delta\mathcal{G}) - \delta\mathcal{G} + f\left(\delta\widetilde{\mathcal{G}}\right) \\ &= \mathcal{W} + \mathcal{G} - \delta\mathcal{G} + f\left(\delta\widetilde{\mathcal{G}}\right) \\ &= \mathcal{R} - \delta\mathcal{G} + f\left(\delta\widetilde{\mathcal{G}}\right). \end{aligned}$$

The left-hand side of this equation is known because we know f, we have observed $\widetilde{\mathcal{R}}$, and we can choose the GIA model we want for G_0 and $\widetilde{\mathrm{G}}_0$. We have no way to separate the terms on the right-hand side, however. As a result, we can readily identify the error we make when computing the pseudo-GRACE product to approximate $\mathcal{R}$:

$$\underbrace{f\left(\widetilde{\mathcal{R}}\right) - f\left(\widetilde{\mathrm{G}}_0\right) + \mathrm{G}_0}_{\text{computed (observed/known)}} = \mathcal{R} + \underbrace{\left[f\left(\delta\widetilde{\mathcal{G}}\right) - \delta\mathcal{G}\right]}_{\text{error (unknown)}}. \tag{10}$$

This error term in eq. (10) is the reason why it is required to introduce two GIA processes and handle them separately for GRACE and GPS data, respectively, in the BHM. Indeed, before computing the actual, GRACE-derived GIA field in terms of VLM, we must first estimate a GIA proxy, or pseudo-GIA, from the pseudo-GRACE product, because the VLM field directly derived from GRACE observations contains an error that we cannot estimate and remove beforehand (eq. 10). On the contrary, we have direct access to VLM using GPS observations. That is why we estimate two GIA fields which we keep separated in the BHM, one for each observation technique. Section 2.3 is dedicated to the detailed description of such an approach.

2.3 Detailed description of the method

For the sake of simplicity, we postpone the discussion of the actual implementation of the method in the BHM to Section 3.1. In this section, we only provide the equations which relate the input data to the processes we want to estimate. Apart from a few assumptions on the estimated fields, we do not need to provide much more information at the physical level anyway as the BHM is strongly data-driven.

In order to avoid more computational complexity than required in the BHM, it is preferable to use linear combinations to relate the processes (GIA and hydrology fields) and the data together. The pseudo-GRACE product makes this constraint easy to satisfy but requires the estimation of two separate GIA fields, one from pseudo-GRACE data, the other from GPS data, as mentioned in Section 2.1.

By analogy with eqs (6) and (7), we define E_1 and E_2, the latent processes of elevation change (VLM), as the sum of hydrology-induced VLM (process W) and GIA-induced VLM for pseudo-GRACE (process G_1) and GPS (process G_2), respectively:

$$\mathrm{E}_1 = \mathrm{W} + \mathrm{G}_1 \quad \text{and} \quad \mathrm{E}_2 = \mathrm{W} + \mathrm{G}_2. \tag{11}$$

It is required to work with deviations from a reference model to fulfil assumptions made in the BHM. That is to say, we must choose an implicit prior and estimate the deviations from a zero mean field for each process. Thus, after subtracting the implicit GIA prior (G_0 of eq. 9b), we actually have

$$\delta\mathrm{E}_1 = \mathrm{W} + \delta\mathrm{G}_1 \quad \text{and} \quad \delta\mathrm{E}_2 = \mathrm{W} + \delta\mathrm{G}_2, \tag{12}$$

where we have defined $\delta\mathrm{E}_i = \mathrm{E}_i - \mathrm{G}_0$ and $\delta\mathrm{G}_i = \mathrm{G}_i - \mathrm{G}_0$ for $i = 1, 2$.

Then, $\delta\mathrm{E}_1$ and $\delta\mathrm{E}_2$ are related to pseudo-GRACE and GPS data ($\mathfrak{Z}$), respectively, as:

$$\begin{aligned} f\left(\widetilde{\mathcal{R}} - \widetilde{\mathrm{G}}_0\right) &= \frac{1}{|\mathcal{F}_i|}\int_{\mathcal{F}_i} \delta\mathrm{E}_1 \, \mathrm{d}s + \epsilon_{\mathcal{R}} \\ &= \langle\delta\mathrm{E}_1\rangle + \epsilon_{\mathcal{R}} \\ &= \langle\mathrm{W} + \delta\mathrm{G}_1\rangle + \epsilon_{\mathcal{R}} \end{aligned} \tag{13}$$

$$\begin{aligned} \mathfrak{Z} - \mathrm{G}_0 &= \delta\mathrm{E}_2 + \epsilon_{\mathfrak{Z}} \\ &= \mathrm{W} + \delta\mathrm{G}_2 + \epsilon_{\mathfrak{Z}}, \end{aligned} \tag{14}$$

with $\epsilon_{\mathcal{R}}$ and $\epsilon_{\mathfrak{Z}}$ the observations errors, $\mathcal{F}_i \in \mathcal{F}$, an ordered set of GRACE footprints and we have replaced the integral for the computation of the average over a footprint with the shorthand notation $\langle . \rangle$. The integral in eq. (13) comes from the areal nature of GRACE data. We need to compute the mean effect of the elevation change process over the corresponding GRACE footprint $\mathcal{F}_i$, taken from all GRACE footprints $\mathcal{F}$, which matches the current location in the estimated field. Note that, because of the linearity of f, $f(\widetilde{\mathcal{R}} - \widetilde{\mathrm{G}}_0)$ is simply the pseudo-GRACE product given in eq. (10), after the removal of the GIA prior G_0.

This formulation, illustrated in Fig. 1, option (a) is physically correct and can be implemented in a BHM framework relatively easily. Its main limitation is that we have to transform $\delta\mathrm{G}_1$ into a geophysically meaningful quantity and eventually (but not necessarily) combine it with $\delta\mathrm{G}_2$ post-BHM. It can be seen in eq. (13) that $\delta\mathrm{G}_1$ is actually estimated from $f(\delta\widetilde{\mathcal{G}})$ when using the pseudo-GRACE approach we have just described, which means that we need to compute $[h \circ f^{-1}](\delta\mathrm{G}_1)$ to get the actual GIA-induced VLM as seen by GRACE.

The strength of this approach, in theory, is that it works equally well when computing an alternative pseudo-GRACE product in which we favour GIA over hydrology, by transforming the original GRACE observations assuming a viscous-only response, using h instead of f (option (b) on Fig. 1). Then, instead of eqs (13) and (14), we would have

$$h\left(\widetilde{\mathcal{R}} - \widetilde{\mathrm{G}}_0\right) = \langle\mathrm{W}_1 + \delta\mathrm{G}\rangle + \epsilon_{\mathcal{R}} \tag{15}$$

$$3 - \mathrm{G}_0 = \mathrm{W}_2 + \delta\mathrm{G} + \epsilon_3, \tag{16}$$

where we have introduced two hydrology processes, W_1 and W_2, and replaced $\delta\mathrm{G}_1$ and $\delta\mathrm{G}_2$ with a single GIA process δG. The practical limitation with this alternative formulation is that the BHM needs to handle two time-evolving processes in that case, which is a more challenging problem and does not yield satisfying results here. As a result, we retain only option (a) given by eqs (13) and (14).

3 APPLICATION

3.1 Bayesian hierarchical modelling in a nutshell

In Section 2.3, we have loosely introduced several processes without specifying how they would be mathematically defined and actually implemented. We address these important questions now. Our data-driven approach is built on a Bayesian hierarchical modelling (BHM) approach for obtaining simultaneous spatio-temporal solutions which is extensively explained in Cressie & Wikle (2011), Zammit-Mangion *et al.* (2015) and Sha *et al.* (2018). Here, we only give a brief summary of our assumptions and choices.

From the BHM perspective, a process is any physical quantity (a field) describing one specific aspect of some multi-faceted geophysical phenomenon. For example, as we have discussed in Section 1.2, GIA can be seen as both a mass change and VLM field but GIA-related VLM and GIA-related mass change are two different processes in the sense of the BHM. As explained in Section 2, we focus on VLM fields in this study. Thus, to avoid unwieldy naming, we may sometimes refer to the GIA-induced VLM field as GIA field and to hydrology-induced VLM field as hydrology field, given that there is no ambiguity. Similarly, we may use the terms PDSML and hydrology interchangeably as all of the PDSML signal is assumed to originate from hydrology in the present context (including present-day snow and ice melting, as mentioned in Section 1.2).

We work with separable space–time fields: each of them will have a description in space [for GIA processes $G_{1,2}(s)$] or space and time [for PDSML process $W(s, t)$]. In space, a process is defined by a Gaussian Markov random field on a mesh, at each vertex of a triangulation which covers the sphere or a subdomain of it. Each process is characterised by a set of hyperparameters, the most relevant in space being its length scale r. This hyperparameter defines the smoothness of the field over the domain. In the BHM, we mostly rely on the difference in smoothness between the VLM field associated with GIA and the VLM field associated with PDSML to separate these processes. Indeed, GIA signal is expected to be much smoother than hydrological signal even if some overlap is expected (see Section 4.3). We have loosely set the prior on hydrology length scale at 10° (or about 1000 km) and the GIA prior at about 40° (4500 km). Once again, these values should be understood as loose thresholds more than tight limits. For example, the spatial length scale prior for hydrology is set in such a way that the probability $P(r > 1000$ km) is small but not zero and, in any case, it is still possible for the hydrology field to exhibit large scale features. In addition, our sensitivity tests have confirmed that we were not sensitive to the choice of priors for the hyperparameters, even when the BHM cannot properly separate the processes (see Section 3.5).

Another essential property of a process is its temporal evolution. Here we define time-invariant processes as those which are constant in time over the observation period and time-evolving those processes which evolve with time. With this convention, the VLM field due to GIA is, at first order, a time-invariant process. On the contrary, VLM due to hydrology cycles is a time-evolving process in general. We assume that the time-evolving processes can be described by an AR(1) model, an autoregressive model of order 1 (for a gentle introduction to the autoregressive model family, see Feigelson *et al.* 2018). For the AR(1) correlation parameter ρ, we assume a fairly uninformative prior by making use of a penalised complexity prior (defined to penalize the complexity induced by deviating from a simpler base model, see Simpson *et al.* 2017). In particular, this prior specifies that the probability $P(\rho > 0)$ is 0.9, that is the probability that the process evolves in time is 0.9. The AR(1) assumption requires that we remove the trend in (pseudo-)GRACE and GPS time-series, which is why we work with VLM instead of displacement. More precisely, we compute the differences between the mean annual displacements for each pair of consecutive years and use these new time-series in the BHM. This operation is similar to the computation of the time derivative with a time step of 1 yr.

As a result, we work with three processes: two time-invariant processes with large spatial length scales which describe the deviation from a GIA forward model ($\delta\mathrm{G}_1$ and $\delta\mathrm{G}_2$) and one time-evolving process which describes the VLM due to PDSML, or hydrology (W), in agreement with eqs (13) and (14). When choosing these processes, we implicitly assume that any other geophysical signal has been removed from the data or is negligible. The validity of this assumption is discussed in Section 4.3.

The spatio-temporal modelling itself, that is the estimation of the VLM fields, involves dedicated statistical techniques which can be found in Lindgren *et al.* (2011).

3.2 Synthetic test

We validate the method and assess its efficiency with a synthetic, or closed-loop test. We focus on North America as it is a comparatively data-rich region, parts of which exhibit a significant GIA signal, and where the underlying processes are relatively well studied and understood. Of course, this choice of region is not important for now as we create synthetic data anyway, but it will become more relevant when using real-world data (Sections 3.4 and 3.5).

We generate a synthetic field made of (1) a positive mass gain over a large region in Alaska, with some overlap of Western Canada, to mimic a deviation from a GIA model and (2) a set of both positive and negative mass change over four regions of various size to mimic trends in hydrology in the conterminous United States. In addition, we put a small hydrological signal on top of the synthetic GIA bulge in Alaska to determine whether it is possible to separate both processes when they are colocated. Then, we compute the corresponding synthetic VLM field, taking into account the geophysical origin of each signal when transforming these mass changes into VLM. To do so, we use the elastic load Love numbers on the hydrological signal (van Dam *et al.* 2007), while the GIA is already in terms of VLM. Note that we do not put any time-evolving component in hydrology in this synthetic test because the extraction of the time-invariant component from a time-evolving field is a trivial problem once all the fields have been properly separated. The real challenge here is to separate GIA from hydrology even when both have a constant, linear trend. These linear trends of the GIA and hydrology components which make up the synthetic VLM field are depicted on Figs 2(a) and (b), respectively.

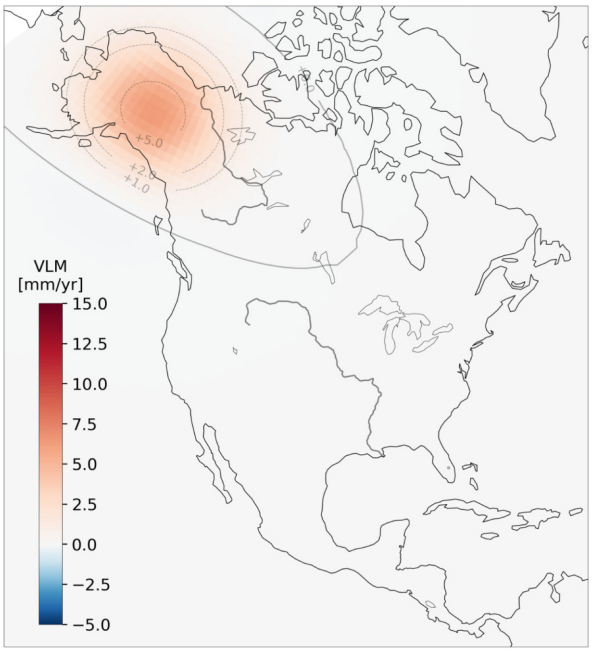

(a) GIA-induced VLM (deviation added to ICE-6G).

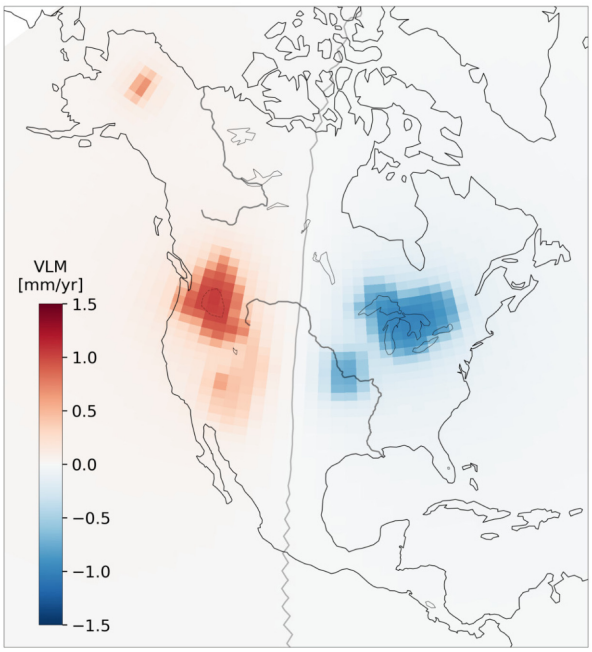

(b) Hydrology-induced VLM.

Figure 2. Synthetic VLM fields used to generate the synthetic data.

The synthetic mass change field is used to generate GRACE data, from which we compute the pseudo-GRACE product by following the procedure described in Section 2.2. The synthetic VLM field is used to generate GPS data, which are simply point samples of the field. Our goal for now is to check the validity of our method, not to assess its practicability on real data. Thus, the density of stations is very loosely chosen to mimic the GPS network over North America, but we simply use a large number of regularly spaced synthetic GPS stations, with a full coverage of the region of interest. In Section 3.4, we suggest a method to improve the coverage to a similar level even when using real data. The linear

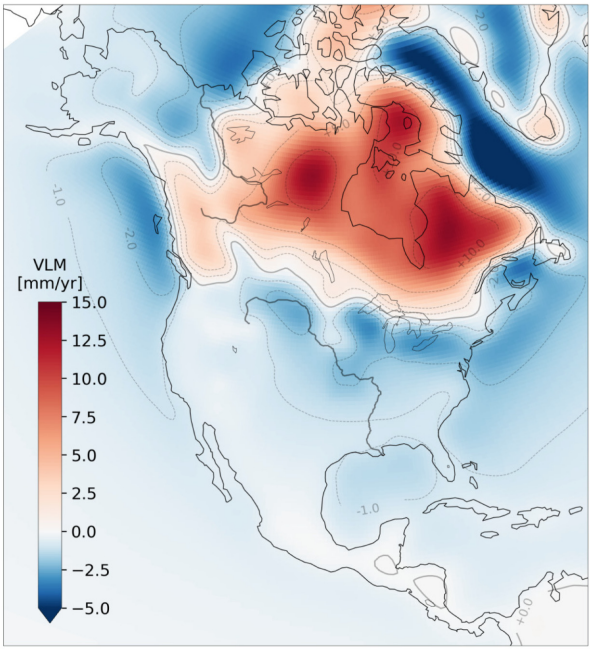

(a) Pseudo-GRACE field. Note the negative patch over the Alaskan-Canadian border due to the mass change-to-VLM transformation of the GIA signal assuming a purely elastic response of the Earth.

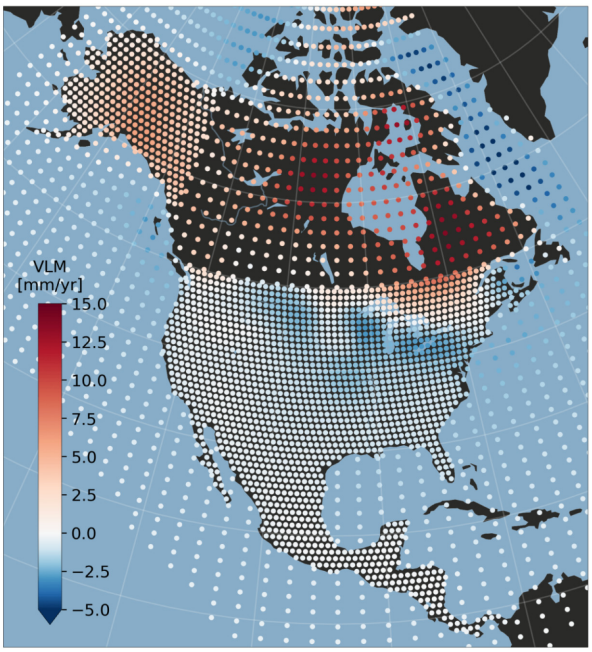

(b) GPS stations used in the synthetic test. In this idealistic case, all the time series are samples of the original VLM field, no virtual stations have been created from pseudo-GRACE data to augment the data (see Sec. 3.4).

Figure 3. Linear trends of the synthetic BHM inputs. The pointed colour bars here and in subsequent figures indicate that the largest or smallest values of the plotted data are beyond the colour bar extrema.

trends of the synthetic pseudo-GRACE field and GPS data set are depicted on Figs 3(a) and (b), respectively. Once the year-to-year difference mentioned in Section 2.3 has been computed, those data sets become the input of the BHM.

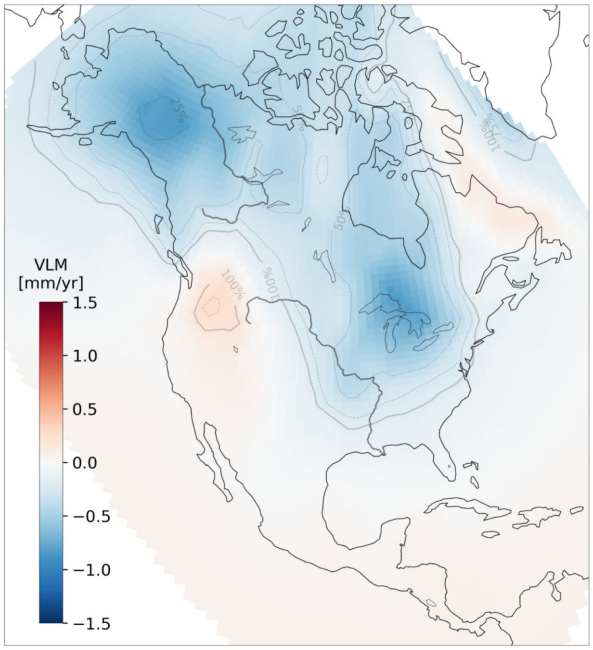

(a) Pseudo-GIA VLM field estimated from pseudo-GRACE data (deviation from ICE-6G).

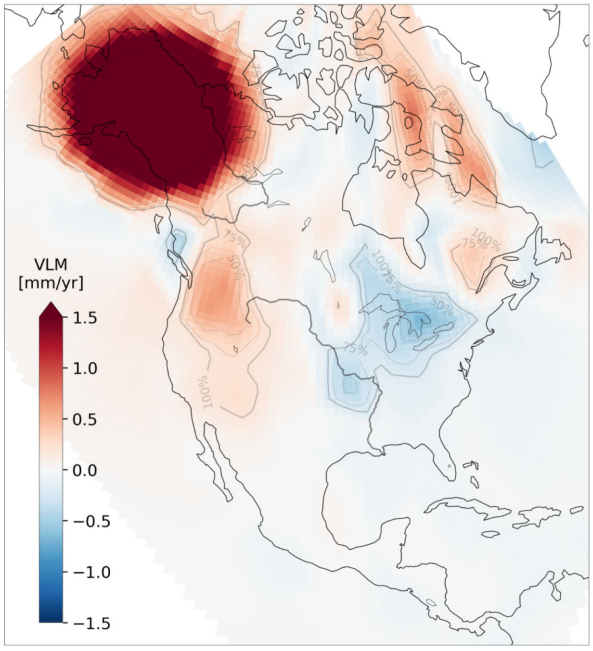

(b) GIA-induced VLM field estimated from GPS data (deviation from ICE-6G). The colour scale is saturated to make the contamination by hydrology visible.

Figure 4. Raw BHM outputs.

3.3 Results of the synthetic test

The output of the BHM for both GIA-induced VLM fields (from pseudo-GRACE and GPS, δG_1 and δG_2) and for the PDSML or hydrology-induced VLM field (W) are depicted on Figs 4(a), (b) and 5, respectively. The VLM field due to PDSML has been split into a time-invariant and a time-evolving component, the latter being zero (and not shown) here, as mentioned in Section 3.2. Thus, only the linear trend is shown on Fig. 5 for hydrology.

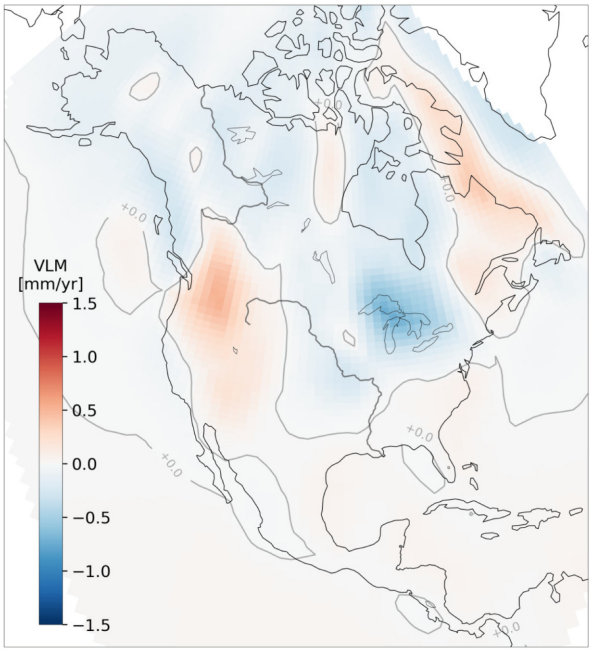

Figure 5. Hydrology-induced VLM field estimated from both GPS and pseudo-GRACE data.

As expected, the VLM field estimated from GPS data for the GIA deviation (δG_1) reveals the additional GIA bulge over Alaska, with both the right shape and amplitude. The maximum uplift amplitude in the original synthetic field and the estimated value in this region are consistent. The second GIA field estimated from pseudo-GRACE data (δG_2) has the same pattern at the correct location but this time the sign is opposite and the amplitude is different, as expected with the pseudo-GRACE data. In brief, this synthetic test confirms that our method enables us to properly extract the GIA deviation from the input data.

Regarding the PDSML-induced VLM field, however, the results are less encouraging as some of the signal is assigned to the GIA fields, as revealed on Figs 4(a) and (b) by the spurious patterns which match our synthetic hydrological signals in the United States. Such contamination was at least partly expected due to the lack of a clear length scale threshold between hydrology and GIA processes. Despite this, most of the hydrological signal is correctly attributed to the PDSML field. Considering that there is also a good match between the hydrology-related patterns in both fields, we can take advantage of these facts to extract the remaining hydrological signals from the GIA field in a post-processing step. A simple method consists in the computation of a scaling factor for the hydrology field and to subtract the scaled version of this field from the GIA field. In so doing, we remove the unwanted hydrology component from the GIA field and we recover a full hydrology field with the expected amplitude. The optimal scaling factor can be determined by minimizing the residuals of the difference between both fields, computed over a restricted region where the fields match in pattern and, to a certain extent, in amplitude. Indeed, in other regions, where a non-zero GIA signal has been identified, the contaminated GIA and the hydrology fields should exhibit different patterns and amplitudes. Obviously, we could use a much more involved method to complement the BHM but the one described appears to be effective as illustrated on Figs 6(a) and (b), which depict the final GIA-induced VLM field and hydrology-induced VLM field, respectively,

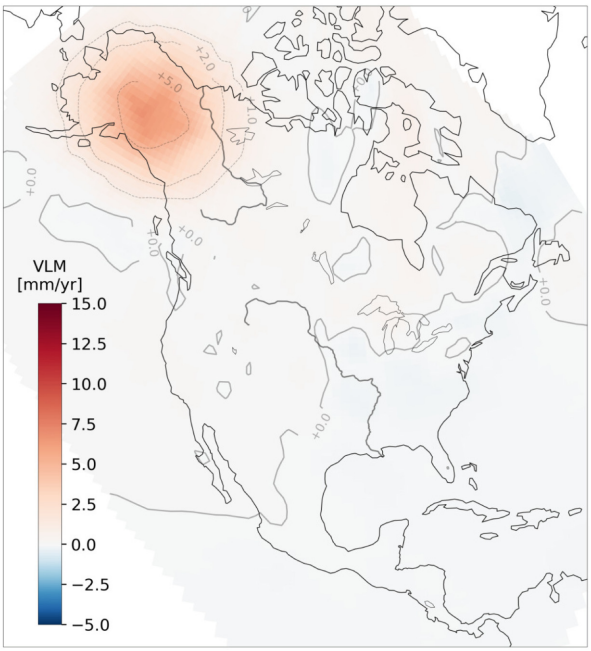

(a) Final GIA-induced VLM field extracted from Fig. 4b (deviation from ICE-6G). To be compared with Fig. 2a.

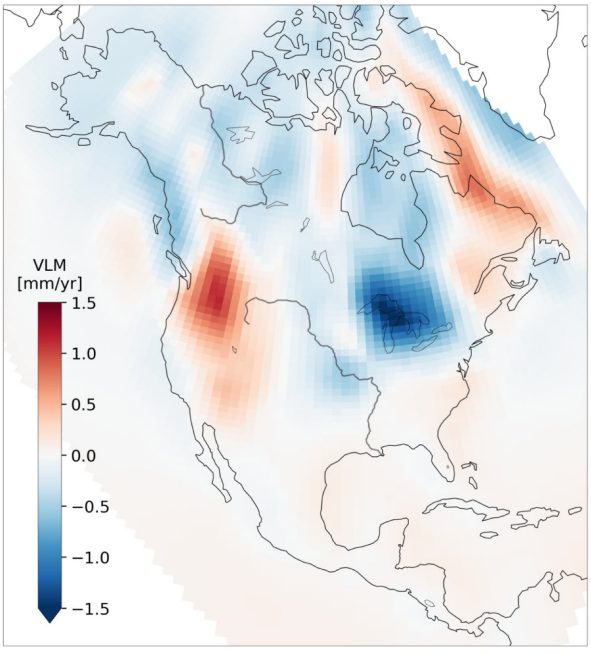

(b) Final hydrology-induced VLM field reconstructed from Fig. 4b and 5. To be compared with Fig. 2b.

Figure 6. Post-processed BHM outputs.

obtained with this technique. These fields can be directly compared with the original synthetic fields used in this closed-loop test, plotted on Fig. 2: there is now a very good agreement overall both in shape and amplitude for all the signals. The result of this qualitative comparison is confirmed by Fig. 7 which depicts the difference between the total VLM field computed from the BHM outputs (plus ICE-6G) and the GPS synthetic data. At large scale, no significant difference is visible and the root-mean-square error (RMSE) is below 0.2 mm yr^{-1}.

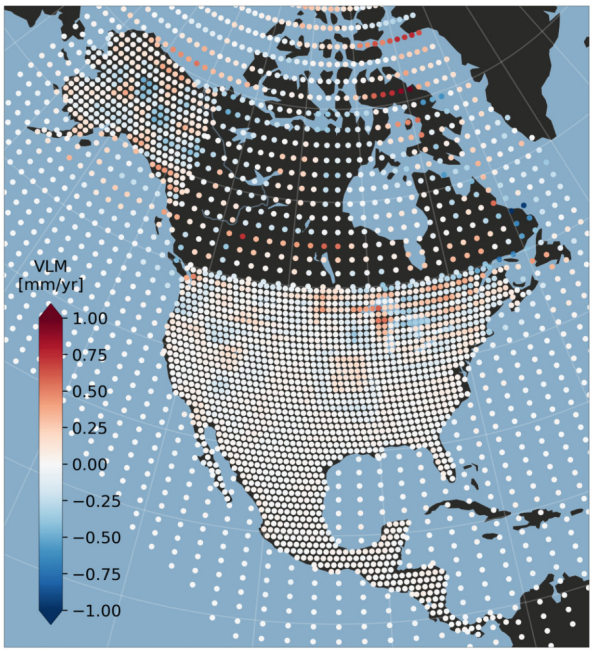

Figure 7. Differences between the total field estimated by the BHM (sum of Figs 6a, b and ICE-6G) and the synthetic trends at each GPS stations from Fig. 3(b). The root-mean-square error computed from these differences is 0.14 mm yr^{-1}.

The most disappointing result is in the region of the small-scale hydrological signal we have superimposed to the GIA signal in Alaska. This discrepancy is confirmed by the differences visible in this region on Fig. 7. Although our method is able to detect this weak signal which was mostly hidden by the much larger GIA uplift, the recovered amplitude is notably smaller than in the original synthetic field. Such discrepancy is not surprising, though, because when both processes occur at the same location, the solution cannot be unique. In the worst case scenario, if GIA and hydrology almost exactly cancel each other, either in terms of mass change or VLM, it becomes impossible to determine the amplitudes of each signal independently in a fully data-driven approach. Similarly, when one of the process strongly dominates (as is the case with GIA in Alaska in this test), we cannot expect the BHM to yield the exact solution for the second, much weaker process. To conclude, the main reason why we are not able to fully extract the hydrological signal colocated with GIA is because of an intrinsic lack of information in the data more than a limitation of the method itself.

3.4 Real data

After validating the method on synthetic data, we now come back to actual observations from GRACE and GPS. Once again, we focus on North America where we expect to have a non-zero linear trend in hydrology superimposed with a GIA signal in some regions. Our period of interest is January 2005 to December 2015. It is a compromise based on the time span of high-quality GRACE observations and the limited GPS data availability prior to 2005.

We use the GPS time-series from the Nevada Geodetic Laboratory (NGL) in the IGS14 reference frame (Blewitt *et al.* 2018), to

which we apply atmospheric loading[1] and polar motion (King & Watson 2014) corrections. The NGL data are provided with a list of possible offset dates at each station, which are associated with earthquakes occurrence and station maintenance. We complement this list using a custom offset detection algorithm, even though this step is not critical as we also inspect all the time-series visually before using them in the BHM, in order to ensure that no large offsets or other problems have been missed. We use a least squares method to estimate the annual, semi-annual and linear trend components at each station, along with the offsets correction modelled by a step function at each assumed offset date. The latter correction is used to remove the offsets before running the BHM. As already mentioned, we assess the overall quality of the resulting data set and discard stations which are outliers, on the basis that they are not representative of the land motion in their region. Indeed, as we are interested in hydrology at regional to continental scale, and in GIA, which is essentially a spatially smooth field, we can safely exclude any station contaminated by a very localized signal, assuming there are enough stations in the surrounding area to identify such abnormal signal. After this last cleaning step, there are approximately 3900 GPS time-series remaining in the final data set. Most of the quality control discussed in this paragraph was undertaken using a new, soon-to-be-released GUI software package dedicated to the visualisation and analysis of a large number of geolocated time-series and initially developed as part of the GlobalMass project.

For the GRACE data, we use the JPL mascon solution available at PODAAC (Watkins *et al.* 2015). These mascon fields are converted to spherical harmonic fields and processed to obtain GRACE products in terms of geopotential and VLM.

In order to properly understand the BHM outputs, we need to further discuss a few important points regarding GPS station selection. There are many regions in North America with geophysical and anthropogenic signals unrelated to GIA or hydrology. Along the Pacific coast, from Alaska to Mexico, several large earthquakes are well-documented, some of them with associated long-term postseismic deformations. Smaller earthquakes which have occurred during our period of study might have impacted GPS observations as well but those time-series with changes in trend associated with an earthquake have been removed. The most potentially problematic events for our study are the 1964 earthquake in southern Alaska, in the Cook Inlet region (Huang *et al.* 2020) and the 2002 Denali fault earthquake in central Alaska (Freed *et al.* 2006). Those have documented postseismic displacements while being located in a region where we expect a non-zero GIA signal. To tackle this problem, there are essentially three different approaches: (1) discarding most if not all of the potentially impacted stations, (2) estimating and applying a correction and (3) keeping as many time-series as possible and trying to separate the sources of the observed signal using other techniques to complement GNSS observations (GRACE here). Option (1) has been used in other works such as in Simon *et al.* (2017), but it would mean that we accept to be blind to all the geophysical processes at play in this region when using our method. Option (2) is the ideal choice but the problem when applying *ad hoc* corrections is that we add another degree of freedom. If the end results are not as expected, it becomes hard to tell whether the limiting factor is in the correction or in the original observations. Conversely, if the results seem to be correct, we cannot tell whether there are no errors or if the errors cancel considering that the estimation of accurate postseismic deformations remains a challenge. That is why our preferred choice is (3), that is to keep most stations and see what the BHM would estimate in those regions with a challenging mix of signals. Note that we have removed all the stations on Kenai Peninsula and others around Cook Inlet anyway, as those where surely dominated by post-seismic signals.

Hydrology-related signals which are not related to surface loading are another family of signals which are incompatible with our assumptions. Indeed, aquifer compaction in some regions of California or anthropogenic water pumping induce VLM and/or mass changes which do not have the signature of a surface load. In a fully data-driven approach, it is useful if not essential to be able to detect when the content of the input data breaks our assumptions. Thus, we have made the choice here to keep stations in regions where a contamination by other signals is expected to see whether the BHM output would reveal these inconsistencies. This logic is in line with our choice regarding stations in Alaska, although we expect the source separation to be even more challenging in the former case.

Like the synthetic data in Section 3.2, the processed GPS and GRACE data are prepared as described in Section 2.3 before being used as inputs of the BHM (ICE-6G removal, pseudo-GRACE product and year-to-year difference computation). In addition, we cluster nearby GPS stations together to decrease the number of data points, increase the signal-to-noise ratio and mitigate spatial correlation problems (except in Alaska and especially in Canada where the density of stations is smaller, compared with the contiguous United States, and the majority of the stations are too isolated to be clustered). Since the data set is very sparse in some regions, we augment it with artificial GPS stations whose time-series are computed from pseudo-GRACE data. Indeed, due to the limitation to the 2005–2015 period, the number of stations in a some areas can be much smaller than the actual number of stations currently—but sometimes recently—installed. This augmentation simply means that pseudo-GRACE data fully determines the field where we have no GPS observations, without having any impact in regions where we have observations. Contrary to the similar approach followed by Vishwakarma *et al.* (2022), where VLM observations were required everywhere to estimate the GIA or hydrology fields, such augmentation is not strictly necessary here, in theory, but it makes the inversion more stable in practice. The resulting data sets are shown on Figs 8(a) and (b) for pseudo-GRACE and GPS, respectively.

3.5 Results with real-world data

The results we obtain from real-world data are shown on Figs 9(a) and (b) for the pseudo-GIA deviation field obtained from pseudo-GRACE data and for the GIA deviation field obtained from GPS data, respectively (these figures are the equivalent of Figs 4(a) and (b) of the synthetic test). The VLM field due to PDSML/hydrology is shown on Fig. 10 (equivalent to Fig. 5 of the synthetic test).

As already noted in the synthetic test, the separation of GIA and hydrology by the BHM is not immediately perfect. We can clearly see some common patterns in the estimated GIA and hydrology fields. Contrary to the synthetic test, however, the fields are much noisier and their correlation is not sufficient to apply the post-BHM processing method described in Section 3.3 to complete the processes separation. We expected the augmentation of the GPS data to mitigate this problem but it seems to be insufficient here. If we complete the separation process anyway, the RMSE, which was at the level of a few tenth of a millimetre per year for the synthetic

[1] MERRA2 atmospheric model (Gelaro *et al.* 2017) provided by the Loading Service (Petrov 2015): http://massloading.net/atm/index.html.

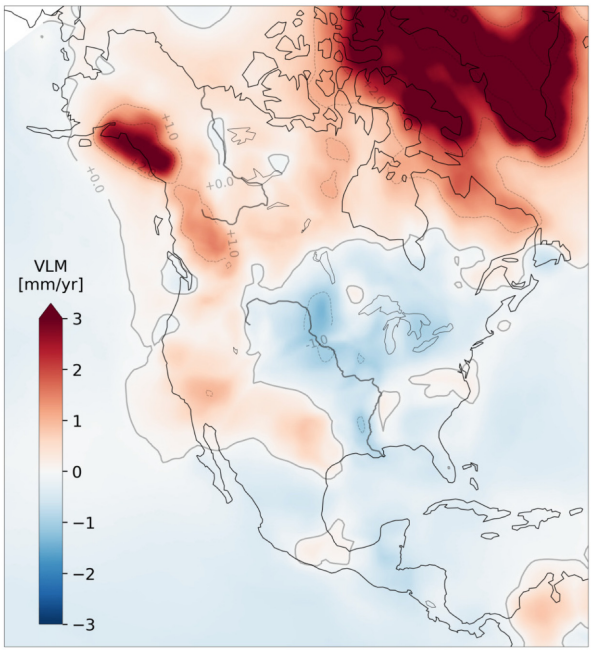

(a) Pseudo-GRACE field (deviation from ICE-6G).

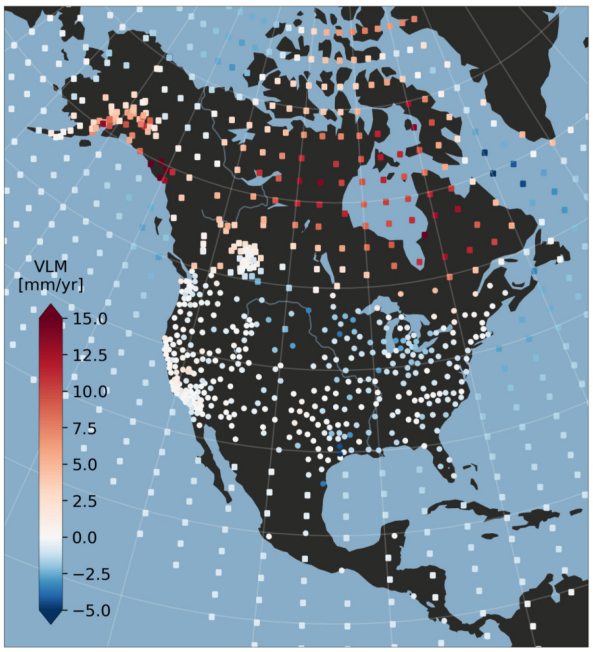

(b) GPS clusters (dots, created from actual GPS stations), GPS stations (for Alaska and Canada, see main text) and virtual stations (squares) generated from pseudo-GRACE data.

Figure 8. Linear trends of the BHM inputs when using actual GRACE and GPS observations.

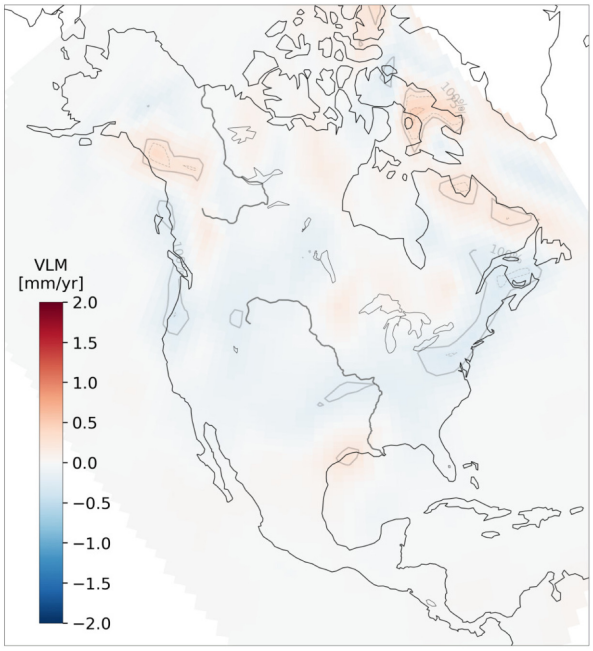

(a) Pseudo-GIA VLM field estimated from pseudo-GRACE data (deviation from ICE-6G).

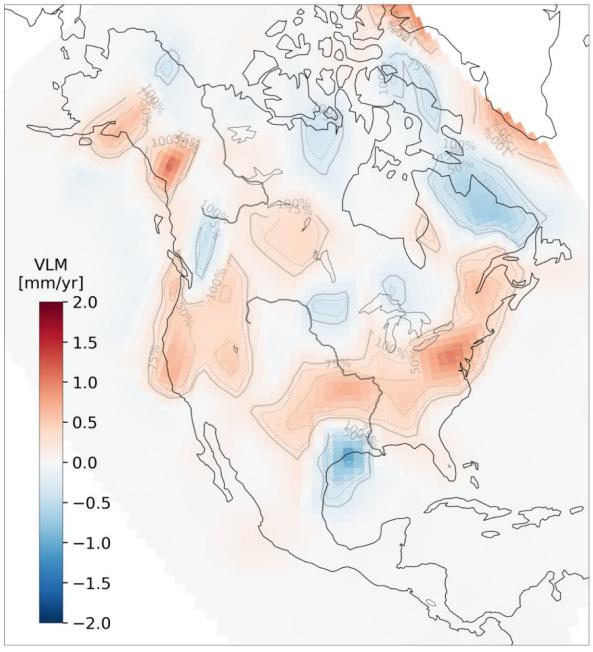

(b) GIA-induced VLM field estimated from GPS data (deviation from ICE-6G).

Figure 9. Raw BHM outputs (linear trend) when using actual GRACE and GPS observations.

test (Section 3.3) is now above 1 mm yr^{-1} with both local and larger scale discrepancies (Fig. 11). The residues are even above 2 mm yr^{-1} for 5 per cent of the stations/clusters. Contrary to the synthetic test, these values are comparable with the differences we would like to estimate.

As a result, it is somewhat difficult to tell which part of the GIA deviation field is an estimate of the deviation from ICE-6G or if a hydrological signal has been wrongly attributed to GIA. Of course, we are confident that the signal in California and most other regions of the conterminous United States is not related to GIA but we can only reach such a conclusion because we have prior geophysical knowledge of the observed signals. In California, we should actually see a negative trend if we had been able to pick the aquifer compaction signal from the stations we have purposely kept in this region (Section 3.4). Because of all these limitations, we cannot provide a reliable geophysical interpretation of Figs 9 and 10.

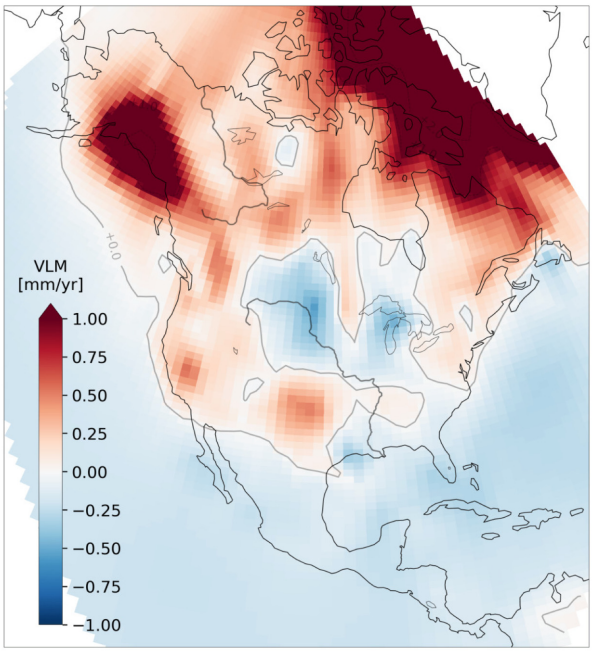

Figure 10. Linear trend of the hydrology-induced field estimated from both pseudo-GRACE and GPS data.

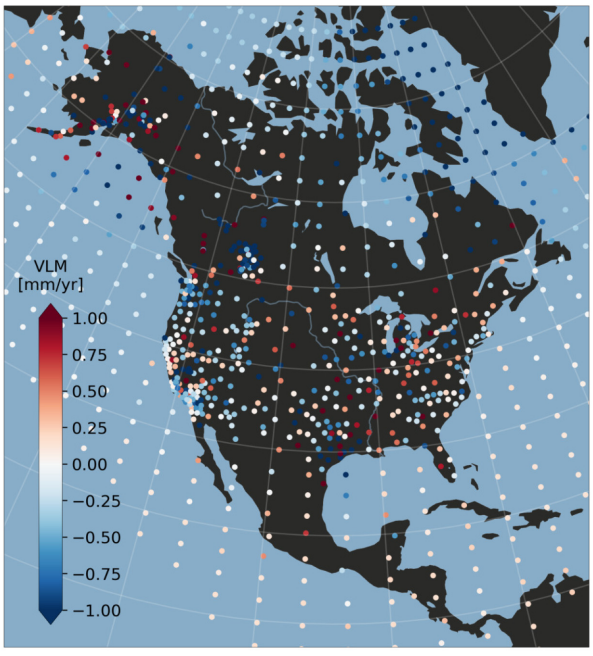

Figure 11. Differences between the total field estimated by the BHM (similar to Fig. 7 for the synthetic test) and the observed trends at the location of each GPS cluster or station from Fig. 8(b). The RMSE computed from these differences is an order of magnitude bigger than the RMSE shown on Fig. 7.

There would be a significant risk of being deceptive if we attempted to determine physical causes for what might only be artefacts due to the aforementioned problems.

We discuss probable reasons for the separation not being as good as the synthetic test when using real-world data and suggest possible improvements in Section 4.2.

Looking at the time-evolving component of the hydrology-induced VLM (Fig. 12), the BHM performs well here with real-world data. This was expected because the separation of a time-evolving signal from all the other time-invariant components is a straightforward task. Nevertheless, we mention this result because such separation is not hard-coded in the BHM like in other methods where the linear trend is explicitly extracted from the time-series. From a purely geophysical point of view, the results depicted on Fig. 12 are also interesting because they give a clear picture of the evolving hydrology in North America over the 2005–2015 period.

4 DISCUSSION

4.1 Data-driven solution to the source separation problem

The closed-loop test discussed in Sections 3.2 and 3.3 has confirmed that the method developed in this study and applied in a BHM framework, complemented by a few simple, assumption-free, post-processing steps, is a successful data-driven approach to separate past and present-day surface loading. This approach is also physically consistent in the sense that it does not require any non-physical assumption on the observed signals and correctly deals with the error made when transforming GRACE data from mass change into VLM. The only issue is the contamination of the GIA fields by some of the PDSML signal but, as we have shown in Section 3.3, there is a way of mitigating this problem when it occurs.

As mentioned in Section 3.3, in regions where one process dominates, the quality of the partitioning of observed VLM between past and present surface loading is primarily determined by the quality of the input data, including the quality of their coverage. However, in regions where both processes are colocated, such as the Great Lakes region (Argus *et al.* 2020), our approach is limited by its data-driven nature, like any other similar approach (see Section 4.3). In theory, we are still able to extract a small signal hidden in a signal of much larger amplitude, but the estimated amplitude of the former is not reliable and the overall quality of the solution will strongly depend on the characteristics of the original signals in such a case, not just on the quality of the observations.

As a result, the answer to the main question of this study—is it possible to separate past and present-day surface loading from GPS and GRACE data in a BHM led data-driven approach?—is ‘yes’ where GIA and hydrology signals are not colocated and when enough observations are available, and the answer is ‘partly’ where both processes are superimposed. A few more conditions are required for this positive conclusion to hold in practice, though, as we shall detail in the next two subsections.

4.2 Challenges and potential improvements

We have established the validity of our approach at the theoretical level, at least when the processes we want to separate do not significantly overlap. Nevertheless, when applying this method to actual observations in North America, we have seen that the quality of the results was not adequate. The most obvious explanation is that we are limited by the density of GPS stations in practice, especially in northern regions. Even if we have improved the coverage with artificial GPS stations, their time-series are computed from pseudo-GRACE data, which means that we cannot estimate a GIA deviation where no GPS stations are present. In those regions where data coverage is very poor, our approach does not perform better than other techniques such as the one used in Vishwakarma

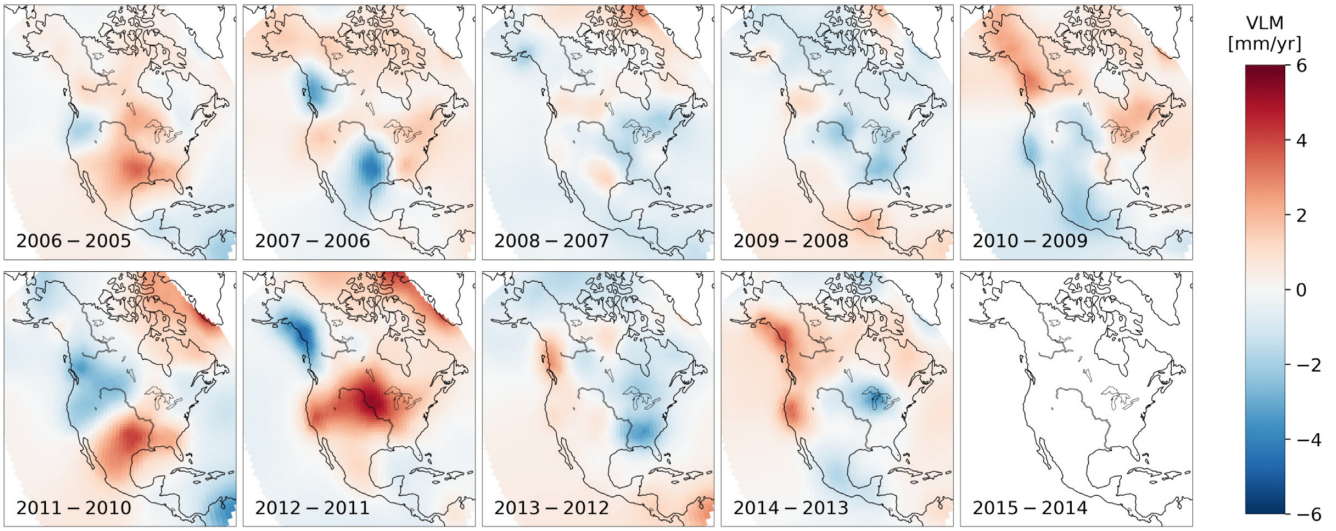

Figure 12. Time-evolving hydrology-induced VLM field estimated by the BHM.

et al. (2022) because the lack of informative data cannot be easily compensated for in a fully data-driven approach without providing additional observations. With the progressive increase in the number of GPS stations, however, this method should yield better results in the near future.

Another potential problem of the current approach when using real data is the contamination of the GIA signal by ice mass change. Indeed, VLM due to present-day mass loss (especially here from the Greenland ice sheet) and VLM due to GIA, are both characterized by a linear trend in time at first order and large length scale in space. Thus, we would ideally need to subtract an ice loading correction from both GPS and GRACE data as we cannot expect the BHM to be able to fully separate both components. We made several attempts to solve that problem but encountered a few major difficulties. First, such an ice correction might depend on GRACE observations, meaning that the same set of observations is used twice in the estimate: once as a correction and once as an input data set. In such a case, these corrections may also depend on the GIA model used to compute them. This problem can be mitigated by using altimetry products to estimate the ice loading correction but there are still assumptions and uncertainties on firn compaction or ice density when doing the volume to mass conversion. Overall, there is still a significant risk that our GIA estimate is biased by the ice correction. In regions where the error on the ice signal is larger than the GIA deviation we are estimating, applying the correction might be worse than simply relying on the BHM to separate the processes. Our attempts at running the BHM after removing the VLM due to present-day ice mass loss from GPS and GRACE observations have shown that at least some of the previous problems were occurring, the ice correction creating several spurious artefacts in the final GIA deviation field, especially in Alaska where all the contributing processes to VLM are difficult to separate.

The last challenge is not related to the method itself but to the implicit assumptions we made when designing our model: possibly the most obvious limitation here is that we have ignored all the processes which are neither related to PDSML/hydrology nor GIA. Even if we have manually excluded many GPS stations in regions affected by tectonics or impacted by local anthropogenic effects, some of the time-series may still contains signals which are not part of our model. Some of them, like tectonics or poroelasticity, can be modelled and removed from the observations but it would be more in line with the approach described in this work to estimate additional processes for these ignored components. The physical complexity of these processes cannot be overlooked, though, and including them in the BHM framework would be an interesting but challenging problem.

4.3 Caveats

In Section 4.1, we have mostly discussed the overall strengths and efficiency of our method. Like any other method, however, it also has a few limitations and pitfalls that we list below. The following points are more generic than the ones discussed in Section 4.2 and should be considered even if other data sets are used.

In Bayesian methods, it is common, if not critical, to assess and discuss the sensitivity to the prior. In the BHM, the actual prior is, strictly speaking, a Gaussian distribution with zero mean, not the GIA forward model from which we estimate a deviation. That is why we called these GIA models *implicit* priors when referring to them from the BHM point of view. We have tried to change the parameters defining these prior distributions (standard deviations); the clear conclusion is that our results are insensitive to these changes. Furthermore, any time we changed the BHM inputs, we got notably different outputs without being restricted by the prior. In other words, the outputs of the BHM are not sensitive to the prior and the results are strongly data-driven as claimed. That being said, we are sensitive to the choice of GIA forward model, because it is used implicitly to define the zero mean of the prior distribution. In Bayesian methods, we cannot reasonably expect the results to be fully independent from the mean of the prior distribution considering that this value determines the position of the domain, in the parameter space, where the solutions will be sought out. If we want physically sensible solutions (or any solution at all), we always need to pick a reasonable domain to explore unless the data are extremely informative. With this comment in mind, it is obvious that we cannot expect to completely get rid of the sensitivity to GIA models. In particular, we cannot expect to get the same results if we change the mean field too much because GRACE has a limited resolution and GPS data are sparse in the region of largest GIA signal.

Another important aspect of the approach is the assumption we make about the spatio-temporal characteristics of the fields we want

to separate (see Section 1.1). The key assumption is that the GIA deviation field is significantly smoother spatially than the PDSML field. In other words, the use of a purely data-driven approach in this context means that we cannot separate processes which exhibit both the same spatial (long) wavelengths and similar temporal behaviour, such as a constant linear trend. Such an assumption on the difference in length scale can be justified by differences in the surface load and by the Earth rheological properties, but the fact that we have to work in terms of VLM implies that the PDSML-induced VLM field is also quite smooth, contrary to what we would have if we were working with changes in EWH. As a reminder, we have chosen to work with VLM because the transformation from mass change to VLM of GRACE data is more robust than the inverse transformation—from VLM to mass change—of sparse GPS data (see Section 2.2). The drawback of this choice is that we are making the difference between GIA and hydrology fields less clear-cut. Of course, it is the result of a trade-off between what can be done with the available data and the physical constraints coming from the model and its implementation.

The last, but most prominent limitation of this work, is also its strength: as we use a fully data-driven approach, our results are essentially limited by the availability and quality of data. In essence, any data-driven approach cannot provide more information than what is actually provided by the data. This means that both the content of the data (signal-to-noise ratio) and their coverage play an important role. Such characteristics are obviously critical in any method but in a data-driven approach, a lack in the data cannot be easily counterbalanced by the constraints coming from the underlying geophysical models. In particular, data gaps in space and time are a limiting factor of our method, even when using time-series of high quality.

5 CONCLUSION

The separation of past and present-day surface loading is a complex challenge which requires a rigorous theoretical framework and dense, high-quality observations. We have shown that it is indeed feasible in theory to partition GIA and PDSML using GPS and GRACE data, following a fully data-driven approach to simultaneously estimate the VLM fields due to each process. In practice, we are limited by the sparsity of GPS stations, especially in Canada and northern Alaska.

The impact of contemporary ice mass loss at large length scale and the local impact of other processes such as tectonics are another difficulty that we can partially overcome when selecting and preprocessing the input data, but which would require a dedicated solution to be tackled at the BHM level, if possible.

ACKNOWLEDGMENTS

AB, JLB, RW, SC, SR and YZ were supported by European Research Council (ERC) under the European Union's Horizon 2020 research and innovation program under grant agreement No. 694188, the GlobalMass project (globalmass.eu). JLB was additionally supported through a Leverhulme Trust Fellowship (RF-2016-718) and a Royal Society Wolfson Research Merit Award. BDV was supported by the Marie Skłodowska-Curie Actions Individual Fellowship (MSCA-IF) under grant agreement no 841407 (CLOSeR).

DATA AVAILABILITY

The authors are grateful for the open availability of observational data sets. The source of each data set is cited in the main text. GRACE data are available at https://podaac.jpl.nasa.gov/. GIA data are available at https://www.atmosp.physics.utoronto.ca/~peltier/data.php by Peltier *et al.* (2015). GPS data are made available by Nevada Geodetic Laboratory. We would make the data and code available to users upon reasonable request.

REFERENCES

Adusumilli, S., Borsa, A.A., Fish, M.A., McMillan, H.K. & Silverii, F., 2019. A decade of water storage changes across the contiguous united states from GPS and satellite gravity, *Geophys. Res. Lett.,* **46**(22), 13 006–13 015.

Argus, D.F. *et al.*, 2020. Rise of great lakes surface water, sinking of the upper Midwest of the United States, and viscous collapse of the Forebulge of the former Laurentide ice sheet, *J. geophys. Res.,* **125**(9), doi:10.1029/2020jb019739.

Blewitt, G., Hammond, W. & Kreemer, C., 2018. Harnessing the GPS data explosion for interdisciplinary science, *EOS,* **99** , doi:10.1029/2018eo104623.

Booker, D., Clarke, P.J. & Lavallée, D.A., 2014. Secular changes in earth's shape and surface mass loading derived from combinations of reprocessed global GPS networks, *J. Geod.,* **88**(9), 839–855.

Chao, B.F., 2016. Caveats on the equivalent water thickness and surface Mascon solutions derived from the GRACE satellite-observed time-variable gravity, *J. Geod.,* **90**(9), 807–813.

Clayton, L. & Moran, S.R., 1982. Chronology of late Wisconsinan glaciation in middle North America, *Quater. Sci. Rev.,* **1**(1), 55–82.

Cressie, N. & Wikle, C.K., 2011. *Statistics for Spatio-Temporal Data,* John Wiley & Sons.

Dyke, A.S., 2004. An outline of North American deglaciation with emphasis on central and northern Canada, in *Quaternary Glaciations-Extent and Chronology - Part II: North America,* pp. 373–424, Elsevier.

Farrell, W.E., 1972. Deformation of the Earth by surface loads, *Rev. Geophys.,* **10**(3), 761 , doi:10.1029/rg010i003p00761.

Feigelson, E.D., Babu, G.J. & Caceres, G.A., 2018. Autoregressive times series methods for time domain astronomy, *Front. Phys.,* **6** , doi:10.3389/fphy.2018.00080.

Freed, A.M., Bürgmann, R., Calais, E., Freymueller, J. & Hreinsdóttir, S., 2006. Implications of deformation following the 2002 Denali, Alaska, earthquake for postseismic relaxation processes and lithospheric rheology, *J. geophys. Res.,* **111**(B1) , doi:10.1029/2005jb003894.

Fritsche, M., Döll, P. & Dietrich, R., 2012. Global-scale validation of model-based load deformation of the earth's crust from continental watermass and atmospheric pressure variations using GPS, *J. Geodyn.,* **59–60,** 133–142.

Gelaro, R. *et al.*, 2017. The Modern-Era Retrospective Analysis for Research and Applications, Version 2 (MERRA-2). *Journal of Climate,* **30**(14).

Geruo, A., Wahr, J. & Zhong, S., 2012. Computations of the viscoelastic response of a 3-D compressible earth to surface loading: an application to glacial isostatic adjustment in Antarctica and Canada, *Geophys. J. Int.,* **192**(2), 557–572.

Gunter, B.C., Didova, O., Riva, R. E.M., Ligtenberg, S. R.M., Lenaerts, J. T.M., King, M.A., van den Broeke, M.R. & Urban, T., 2014. Empirical estimation of present-day Antarctic glacial isostatic adjustment and ice mass change, *Cryosphere,* **8**(2), 743–760.

Hu, Y. & Freymueller, J.T., 2019. Geodetic observations of time-variable glacial isostatic adjustment in southeast Alaska and its implications for Earth rheology, *J. geophys. Res.,* **124**(9), 9870–9889.

Huang, K., Hu, Y. & Freymueller, J.T., 2020. Decadal viscoelastic postseismic deformation of the 1964 Mw9.2 Alaska earthquake, *J. geophys. Res.,* **125**(9), doi:10.1029/2020jb019649.

Husson, L., Bodin, T., Spada, G., Choblet, G. & Kreemer, C., 2018. Bayesian surface reconstruction of geodetic uplift rates: mapping the global fingerprint of glacial isostatic adjustment, *J. Geodyn.,* **122,** 25–40.

King, M.A. & Watson, C.S., 2014. Geodetic vertical velocities affected by recent rapid changes in polar motion, *Geophys. J. Int.,* **199**(2), 1161–1165.

Li, T. *et al.*, 2020. Uncertainties of glacial isostatic adjustment model predictions in North America associated with 3D structure, *Geophys. Res. Lett.,* **47**(10), doi:10.1029/2020gl087944.

Lindgren, F., Rue, H. & Lindström, J., 2011. An explicit link between Gaussian fields and Gaussian Markov random fields: the stochastic partial differential equation approach, *J. R. Stat. Soc.,* **73,** 423–498.

Margold, M., Stokes, C.R. & Clark, C.D., 2018. Reconciling records of ice streaming and ice margin retreat to produce a palaeogeographic reconstruction of the deglaciation of the Laurentide ice sheet, *Quater. Sci. Rev.,* **189,** 1–30.

Marsman, C.P., van der Wal, W., Riva, R. E.M. & Freymueller, J.T., 2021. The impact of a 3-D earth structure on glacial isostatic adjustment in southeast Alaska following the little ice age, *J. geophys. Res.,* **126**(12),.

Martín-Español, A. *et al.*, 2016. Spatial and temporal Antarctic Ice Sheet mass trends, glacio-isostatic adjustment, and surface processes from a joint inversion of satellite altimeter, gravity, and GPS data, *J. geophys. Res.,* **121**(2), 182–200.

Nordman, M., Mäkinen, J., Virtanen, H., Johansson, J.M., Bilker-Koivula, M. & Virtanen, J., 2009. Crustal loading in vertical GPS time series in fennoscandia, *J. Geodyn.,* **48**(3–5), 144–150.

Peltier, W.R., 1974. The impulse response of a Maxwell Earth, *Rev. Geophys.,* **12**(4), 649 , doi:10.1029/rg012i004p00649.

Peltier, W.R., Argus, D.F. & Drummond, R., 2015. Space geodesy constrains ice age terminal deglaciation: the global ICE-6g_c (VM5a) model, *J. geophys. Res.,* **120**(1), 450–487.

Petrov, L. The International Mass Loading Service 2015 arXiv

Rietbroek, R., Brunnabend, S.-E., Kusche, J., Schröter, J. & Dahle, C., 2016. Revisiting the contemporary sea-level budget on global and regional scales, *PNAS,* **113**(6), 1504–1509.

Riva, R.E.M. *et al.*, 2009. Glacial Isostatic Adjustment over Antarctica from combined ICESat and GRACE satellite data, *Earth planet. Sci. Lett.,* **288**(3), 516–523.

Rue, H., Martino, S. & Chopin, N., 2009. Approximate Bayesian inference for latent Gaussian models by using integrated nested Laplace approximations, *J. R. Stat. Soc., B,* **71**(2), 319–392.

Schumacher, M., King, M.A., Rougier, J., Sha, Z., Khan, S.A. & Bamber, J.L., 2018. A new global GPS data set for testing and improving modelled GIA uplift rates, *Geophys. J. Int.,* **214**(3), 2164–2176.

Sella, G.F., Stein, S., Dixon, T.H., Craymer, M., James, T.S., Mazzotti, S. & Dokka, R.K., 2007. Observation of glacial isostatic adjustment in "stable" North America with GPS, *Geophys. Res. Lett.,* **34**(2) , doi:10.1029/2006gl027081.

Sha, Z., Rougier, J.C., Schumacher, M. & Bamber, J.L., 2018. Bayesian model-data synthesis with an application to global glacio-isostatic adjustment, *Environmetrics,* **30**(1), e2530 , doi:10.1002/env.2530.

Simon, K., Riva, R., Kleinherenbrink, M. & Tangdamrongsub, N., 2017. A data-driven model for constraint of present-day glacial isostatic adjustment in North America, *Earth planet. Sci. Lett.,* **474,** 322–333.

Simpson, D., Rue, H., Riebler, A., Martins, T.G. & Sørbye, S.H., 2017. Penalising model component complexity: a principled, practical approach to constructing priors, *Stat. Sci.,* **32**(1) , doi:10.1214/16-sts576.

Tapley, B.D. *et al.*, 2019. Contributions of GRACE to understanding climate change, *Nat. Clim. Change,* **9,** 358–369.

Tregoning, P., Watson, C., Ramillien, G., McQueen, H. & Zhang, J., 2009. Detecting hydrologic deformation using GRACE and GPS, *Geophys. Res. Lett.,* **36**(15), doi:10.1029/2009gl038718.

van Dam, T., Wahr, J. & Lavallée, D., 2007. A comparison of annual vertical crustal displacements from GPS and gravity recovery and climate experiment (GRACE) over Europe, *J. geophys. Res.,* **112**(B3), doi:10.1029/2006jb004335.

van Dam, T., Wahr, J., Milly, P. C.D., Shmakin, A.B., Blewitt, G., Lavallée, D. & Larson, K.M., 2001. Crustal displacements due to continental water loading, *Geophys. Res. Lett.,* **28,** 651–654.

van der Wal, W., Whitehouse, P.L. & Schrama, E.J., 2015. Effect of GIA models with 3D composite mantle viscosity on GRACE mass balance estimates for Antarctica, *Earth planet. Sci. Lett.,* **414,** 134–143.

van der Wal, W., Wu, P., Sideris, M.G. & Shum, C., 2008. Use of GRACE determined secular gravity rates for glacial isostatic adjustment studies in North America, *J. Geodyn.,* **46**(3–5), 144–154.

Vishwakarma, B.D., Devaraju, B. & Sneeuw, N., 2018. What is the spatial resolution of grace satellite products for hydrology?, *Rem. Sens.,* **10**(852), doi:10.3390/rs10060852.

Vishwakarma, B.D., Ziegler, Y., Bamber, J.L. & Royston, S., 2022. Separating GIA signal from surface mass change using GPS and GRACE data, *Geophys. J. Int.,* in press, doi:10.1093/gji/ggac336.

Watkins, M.M., Wiese, D.N., Yuan, D.-N., Boening, C. & Landerer, F.W., 2015. Improved methods for observing Earth's time variable mass distribution with GRACE using spherical cap Mascons, *J. geophys. Res.,* **120**(4), 2648–2671.

Wu, X. *et al.*, 2010. Simultaneous estimation of global present-day water transport and glacial isostatic adjustment, *Nat.Geosci.,* **3,** 642–646.

Zammit-Mangion, A., Rougier, J., Schön, N., Lindgren, F. & Bamber, J., 2015. Multivariate spatio-temporal modelling for assessing Antarctica's present-day contribution to sea-level rise, *Environmetrics,* **26**(3), 159–177.

APPENDIX: VISHWAKARMA *ET AL.* 2022 APPROACH ADAPTED TO THE BHM

The approach of Vishwakarma *et al.* (2022) mentioned in Sections 1.4 and 2 can be translated for use in our BHM framework. It is more convoluted than the method presented in this work because we must use f and h (see Fig. 1) to transform both some of the observations and some of the processes. In return, its strength is that it is not required to actually do complex computations involving f or h inside the BHM.

Keeping the notations of Section 2, this approach starts from the fact that

$$\begin{aligned}\mathcal{R} - \mathrm{G}_0 &= f\left(\widetilde{\mathcal{R}}\right) - f\left(\widetilde{\mathcal{G}}\right) + h\left(\widetilde{\mathcal{G}}\right) - \mathrm{G}_0 \\ &= f\left(\widetilde{\mathcal{R}} - \widetilde{\mathrm{G}}_0\right) - f(\widetilde{\mathcal{G}} - \widetilde{\mathrm{G}}_0) + h(\widetilde{\mathcal{G}} - \widetilde{\mathrm{G}}_0) \\ &= f\left(\widetilde{\mathcal{R}} - \widetilde{\mathrm{G}}_0\right) - f\left(\delta\widetilde{\mathcal{G}}\right) + h\left(\delta\widetilde{\mathcal{G}}\right), \end{aligned} \tag{A1}$$

Then, eq. (13) is replaced with

$$f\left(\widetilde{\mathcal{R}} - \widetilde{\mathrm{G}}_0\right) = \langle\delta\mathrm{E}\rangle + f\left(\delta\widetilde{\mathcal{G}}\right) - h\left(\delta\widetilde{\mathcal{G}}\right) + \epsilon_{\mathcal{R}}. \tag{A2}$$

Similarly, but focusing now on the hydrology field, we have

$$\mathcal{R} - \mathrm{G}_0 = h\left(\widetilde{\mathcal{R}}\right) - h\left(\widetilde{\mathcal{W}}\right) + f\left(\widetilde{\mathcal{W}}\right) - \mathrm{G}_0, \tag{A3}$$

which leads to

$$h\left(\widetilde{\mathcal{R}} - \widetilde{\mathrm{G}}_0\right) = \langle\delta\mathrm{E}\rangle - f\left(\widetilde{\mathcal{W}}\right) + h\left(\widetilde{\mathcal{W}}\right) + \epsilon_{\mathcal{R}}. \tag{A4}$$

If we introduce a new functional $\chi = f - h$, we can write eqs (A2) and (A4) more succinctly:

$$f\left(\widetilde{\mathcal{R}} - \widetilde{\mathrm{G}}_0\right) = \langle\delta\mathrm{E}\rangle + \chi\left(\delta\widetilde{\mathcal{G}}\right) + \epsilon_{\mathcal{R}} \tag{A5}$$

$$h\left(\widetilde{\mathcal{R}} - \widetilde{\mathrm{G}}_0\right) = \langle\delta\mathrm{E}\rangle - \chi\left(\widetilde{\mathcal{W}}\right) + \epsilon_{\mathcal{R}}. \tag{A6}$$

Here we have a complex computation, using χ, that the BHM cannot handle. In order to avoid it, we may simply define new abstract processes from processes given in terms of changes in EWH ($\delta\widetilde{\mathrm{G}}$ for GIA deviation, $\widetilde{\mathrm{W}}$ for hydrology and $\delta\widetilde{\mathrm{E}} = \widetilde{\mathrm{W}} + \delta\widetilde{\mathrm{G}}$) and work with these new meta-processes:

$$\delta\mathrm{E}_\chi = \chi\left(\delta\widetilde{\mathrm{E}}\right), \mathrm{W}_\chi = \chi\left(\widetilde{\mathrm{W}}\right) \text{ and } \delta\mathrm{G}_\chi = \chi\left(\delta\widetilde{\mathrm{G}}\right). \tag{A7}$$

Then, similarly to eq. (13) but now for both GIA and PDSML, we have

$$\chi\left(\delta\widetilde{\mathcal{G}}\right) = \left\langle \delta \mathrm{G}_{\chi} \right\rangle + \epsilon_{\chi\left(\delta\widetilde{\mathcal{G}}\right)} \tag{A8}$$

$$\chi\left(\widetilde{\mathcal{W}}\right) = \left\langle \mathrm{W}_{\chi} \right\rangle + \epsilon_{\chi\left(\widetilde{\mathcal{W}}\right)} \tag{A9}$$

and, considering that $\langle x \rangle + \langle y \rangle = \langle x + y \rangle$, we can rewrite eqs (A5) and (A6) as

$$f\left(\widetilde{\mathcal{R}} - \widetilde{\mathrm{G}}_0\right) = \left\langle \delta \mathrm{E} + \delta \mathrm{G}_{\chi} \right\rangle + \epsilon'_{\mathcal{R}} \tag{A10}$$

$$h\left(\widetilde{\mathcal{R}} - \widetilde{\mathrm{G}}_0\right) = \left\langle \delta \mathrm{E} - \mathrm{W}_{\chi} \right\rangle + \epsilon''_{\mathcal{R}}, \tag{A11}$$

where we have collated the error terms into $\epsilon'_{\mathcal{R}}$ and $\epsilon''_{\mathcal{R}}$.

In this new formulation, $\langle \delta \mathrm{E} \rangle$ is still related to the GPS data using eq. (14) and, compared with the BHM formulation given in Section 2.3, we have two new processes, δG_{χ} and W_{χ}, which are related to two different pseudo-GRACE products, namely $f(\widetilde{\mathcal{R}} - \widetilde{\mathrm{G}}_0)$ and $h(\widetilde{\mathcal{R}} - \widetilde{\mathrm{G}}_0)$. Note, as a sanity check, that taking the difference between eqs (A10) and (A11) (and neglecting the error terms) gives

$$\begin{aligned} f\left(\widetilde{\mathcal{R}} - \widetilde{\mathrm{G}}_0\right) - h\left(\widetilde{\mathcal{R}} - \widetilde{\mathrm{G}}_0\right) &= \left\langle \chi(\delta\widetilde{\mathrm{G}}) \right\rangle + \left\langle \chi(\widetilde{\mathrm{W}}) \right\rangle \\ \chi\left(\widetilde{\mathcal{R}} - \widetilde{\mathrm{G}}_0\right) &= \left\langle \chi(\delta\widetilde{\mathrm{E}}) \right\rangle \end{aligned}$$

as expected.

One of the problems in this approach is that the processes δG_{χ} and W_{χ} only appear in relation with GRACE data; the BHM is not informed that the GPS data are also sensitive to these processes. In addition, there are two time-evolving processes to estimate here (δE and δW_{χ}), which is more challenging for the BHM, and large regions where we have no GPS data to constrain δE. In the original least squares approach of Vishwakarma *et al.* (2022), the augmented GPS data themselves replace the $\langle \delta \mathrm{E} \rangle$ term in all the previous equations and the unknown processes are directly and independently estimated from eqs (A10) and (A11).